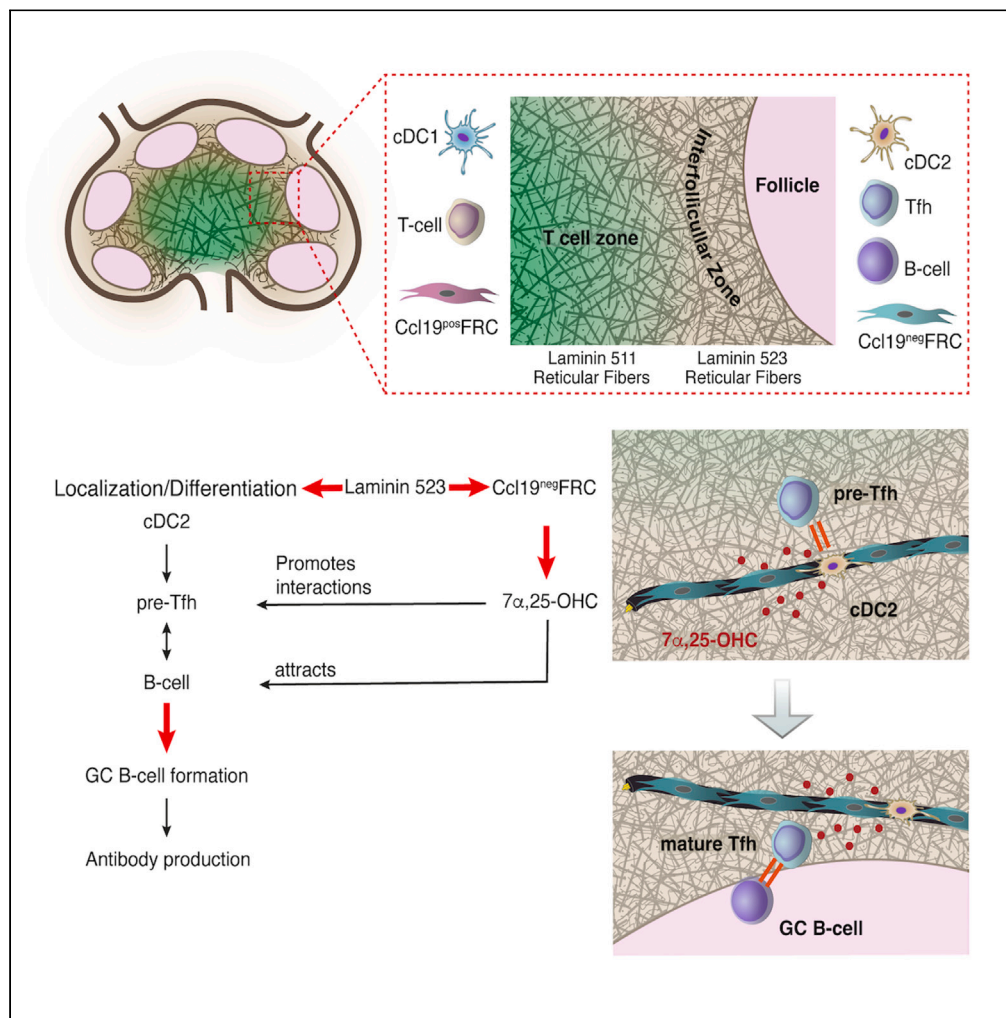**Article**

The extracellular matrix of lymph node reticular fibers modulates follicle border interactions and germinal center formation

Jian Song, Tushar Deshpande, Xueli Zhang, Melanie-Jane Hannocks, Nils Lycke, Susanna L. Cardell, Lydia Sorokin

songj@uni-muenster.de (J.S.)
sorokin@uni-muenster.de (L.S.)

Highlights

Lymph node reticular fiber (RF) extracellular matrix varies at different sites

Loss of RF laminin 523 reduces Tfh- and germinal center (GC) B-cells

Laminin 523 affects follicle-bordering fibroblastic reticular cell phenotype

RF laminin 523 affects cDC2 numbers and localization at follicle borders

Article

The extracellular matrix of lymph node reticular fibers modulates follicle border interactions and germinal center formation

Jian Song,[1,*] Tushar Deshpande,[1] Xueli Zhang,[1,3] Melanie-Jane Hannocks,[1] Nils Lycke,[2] Susanna L. Cardell,[2] and Lydia Sorokin[1,4,*]

SUMMARY

Germinal center (GC) formation and antibody production in lymph node follicles require coordinated interactions between B-cells, T-cells and dendritic cells (DCs), orchestrated by the extracellular matrix-rich reticular fiber (RF) network. We describe a unique laminin 523-containing RF network around and between follicles that associates with PDGFrecβ^{high}CCL19^{low}gp38^{low} fibroblastic reticular cells (FRC). In the absence of FRC expression of laminin α5 (*pdgfrb-cre:Lama5$^{fl/fl}$*), pre-Tfh-cells, B-cells and DCs are displaced from follicle borders, correlating with fewer Tfh-cells and GC B-cells. Total DCs are not altered in *pdgfrb-cre:Lama5$^{fl/fl}$* mice, but cDC2s, which localize to laminin α5 in RFs at follicle borders, are reduced. In addition, PDGFrecβ^{high}CCL19^{low}gp38^{low} FRCs show lower *Ch25h* expression, required for 7α,25-dihydroxycholesterol synthesis that attracts pre-Tfh-cells, B-cells and DCs to follicle borders. We propose that RF basement membrane components represent a type of tissue memory that guides the localization and differentiation of both specialized FRC and DC populations, required for normal lymph node function.

INTRODUCTION

Antibody production to most antigens is T-cell dependent and requires formation of germinal centers (GCs), specialized microenvironments in the B-cell follicles of lymph nodes optimized for induction and maintenance of memory B-cells and long-lived plasma cells.[1] GCs form in response to antigen-specific priming of B-cells by the coordinated interaction of several different cell types, including dendritic cells (DCs), T-cells and B-cells, and relies on precise temporospatial interactions of these cells and their activities. Such interactions are critically affected by the reticular fiber (RF) network which compartmentalizes immune cells in lymph nodes and other lymphoid organs[2] but also acts as a conduit system for the fast delivery of antigens and/or cytokines from the periphery.[3]

GC formation is initiated by antigen presentation by DCs to CD4$^+$T-cells in the lymph node, whereupon a subset of activated CD4$^+$T-cells, the pre-T-follicular helper (Tfh) cells, upregulate CXCR5 and sphingosine-1-phosphate receptor 2 (S1PR2) and downregulate CCR7, which allows them to migrate toward the B-cell follicles where the CXCR5 ligand, CXCL13, is enriched. Antigen stimulation also localizes the B-cells to the border of the B-cell follicle,[4,5] where a dense RF network supports close interaction between the activated B-cells and the pre-Tfh-cells.[6] This also involves several conjugative signals including ICOS/ICOS-L, CD40L/CD40 and CD28/CD86 that determine not only B-cell activation but also T-cell fate.[7,8] Failure to form stable interactions between the pre-Tfh-cells and B-cells at the follicle border leads to impaired Tfh-cell differentiation and ablation of GC formation (reviewed in[9]), highlighting the critical importance of temporospatial interactions between these cells for GC-formation and function.

In addition to fibroblastic reticular cells (FRCs), the RF network is composed of a specialized extracellular matrix (ECM),[3,10] collectively forming a highly flexible structure that compartmentalizes B- and T-cell zones and provides scaffolds for the localization of resident DCs, for immigrating B- and T-cells,[11] and for DCs migrating into the lymph node from the lymphatic sinus.[12] We have previously shown that the ECM of RFs is unusual, consisting of a central core of fibrillar collagens surrounded by a basement membrane-like structure which is enclosed within a layer of interdigitating FRCs and resident DCs.[3] Of interest, the

composition of both the fibrillar collagen core and of the basement membrane layer differs in different immune cell compartments,[2,10] as do markers of the associated FRCs,[13] suggesting a role for RFs beyond the structural and conduit functions that have been described so far.[3,14]

Indeed, FRCs located at the T-/B-cell border in the lymph node have been shown to differ to those of other sites,[13] among other factors these cells express 7α,25-dihydroxycholesterol (7α25-OHC),[15] which attracts antigen-activated B- and CD4$^+$T-cells and helps their positioning at the follicle interface and in the interfollicular zone.[13,15] At this site, CD4$^+$T-cells are primed by CD4$^+$CD25$^+$ cDC2s and, thereby, exposed to Tfh-cell differentiating factors, such as inducible co-stimulator ligand (ICOSL), required for the development of CCR7^{low}ICOS^{high}PD-1^{high}CXCR5^{high} Tfh-cells.[16] The activated B-cells subsequently downregulate the 7α25-OHC receptor, EBI2, resulting in their movement toward the center of the follicle to form the GC.

We have previously shown that the ECM composition of RFs in the marginal zone (MZ) of the spleen contributes to a developmental niche for MZ B-cells important to T-cell independent antibody responses. Commitment to the MZ B-cell lineage is promoted in incoming pre-B-cells by integrin α6β1-mediated interaction with laminin 511, a heterotrimeric molecule composed of laminin α5, β1 and γ1 chains that is enriched in RFs of the MZ.[2] However, mice lacking laminin α5 in RFs of the MZ and marginal sinus also showed a reduced T-cell dependent antigen response,[2] which we were unable to explain at the time. As laminin α5 is also found in lymph node RFs,[2,3] we speculate that it may play a role in GC-dependent antibody production. We, therefore, here employ transgenic mice lacking laminin α5 in RFs (*pdgfrb-cre::Lama5$^{fl/fl}$*) to investigate its function in GC formation.

A dense RF network containing laminin 523, an unusual isoform composed of laminin α5, β2 and γ3 chains, was found around follicles and in the interfollicular areas, the expression of which was lost in *pdgfrb-cre::Lama5$^{fl/fl}$* mice without a change in RF density. In the absence of laminin α5, Tfh-cell numbers were reduced and exhibited reduced location to the T-/B-cell border, resulting in a marked reduction in GC B-cell numbers. Total DC numbers were not altered *pdgfrb-cre:Lama5$^{fl/fl}$* lymph nodes, but CD4$^+$CD25$^+$ cDC2s, which associate with RFs surrounding follicles were reduced. In addition, laminin α5 was shown to promote follicle-border FRC expression of 7α,25-dihydroxycholesterol, required for pre-Tfh-, B-cell and DC attraction to this site and subsequent Tfh-cell commitment.[17–19] Our data reveal that the ECM of RFs affects the differentiation of cDC2s and their localization at follicle borders but that it also contributes to the unique characteristics of follicle-bordering FRCs, thereby, influencing T-cell dependent antibody immune responses.

RESULTS

Immunofluorescence staining of the ECM components and FRC markers

Staining of lymph nodes from non-immunized WT mice for laminin α5 revealed the RF network throughout the T-cell zone (Figure 1A), as we have previously reported.[3] Laminin α5 staining was sparse within B-cell follicles, but dense in the tissue surrounding the B-cell follicles and at the interfollicular regions (Figures 1B and 1C). Staining for other laminin chains revealed enrichment of laminin β1 and β2 around follicles and almost exclusive localization of laminin γ3 around follicles and in some RFs within follicles (Figure 1D). Laminin α5 was significantly reduced in the *pdgfrb-cre::Lama5$^{fl/fl}$* lymph nodes (Figure 1D), with only basement membranes of high endothelial venules (HEVs) and of small arterioles retaining laminin α5 immunoreactivity (Figures 1D and 1E), due to laminin α5 expression by endothelium.[20] Notably, the peri-follicular staining for laminin γ3 was lost in *pdgfrb-cre::Lama5$^{fl/fl}$* lymph nodes and was significantly reduced for laminin β2 (Figure 1D). This suggests the existence of an unusual laminin isoform, laminin 523,[21] surrounding B-cell follicles. Staining for other ECM components of RFs and for FRC markers revealed no differences between WT and *pdgfrb-cre::Lama5$^{fl/fl}$* lymph nodes (Figures S1A and S1B). Although PDGFrecβ staining was even throughout the RF network, gp38 (also known as podoplanin) staining was intense in the T-cell zone and low at follicle borders and in interfollicular areas, as reported also by others[22]; like other FRC markers, gp38 staining ensheathed the inner ECM core of RFs (Figure 1F).[3]

Immune response after NP-CG immunization

To investigate T-cell dependent immune response, we immunized *pdgfrb-cre::Lama5$^{fl/fl}$* and WT mice with NP-CGG and examined lymph nodes at day 7 and 28. To evaluate the number and size of GCs we stained for CD35 and GL-7 in the lymph nodes of immunized *pdgfrb-cre::Lama5$^{fl/fl}$* and WT controls, revealing no overt differences (Figure S2). At day 7, flow cytometry revealed that 3.66% of total CD4$^+$T-cells were PD-1$^+$CXCR5$^+$CD4$^+$ Tfh-cells in WT lymph nodes, whereas only 0.99% were found in *pdgfrb-cre::Lama5$^{fl/fl}$* lymph
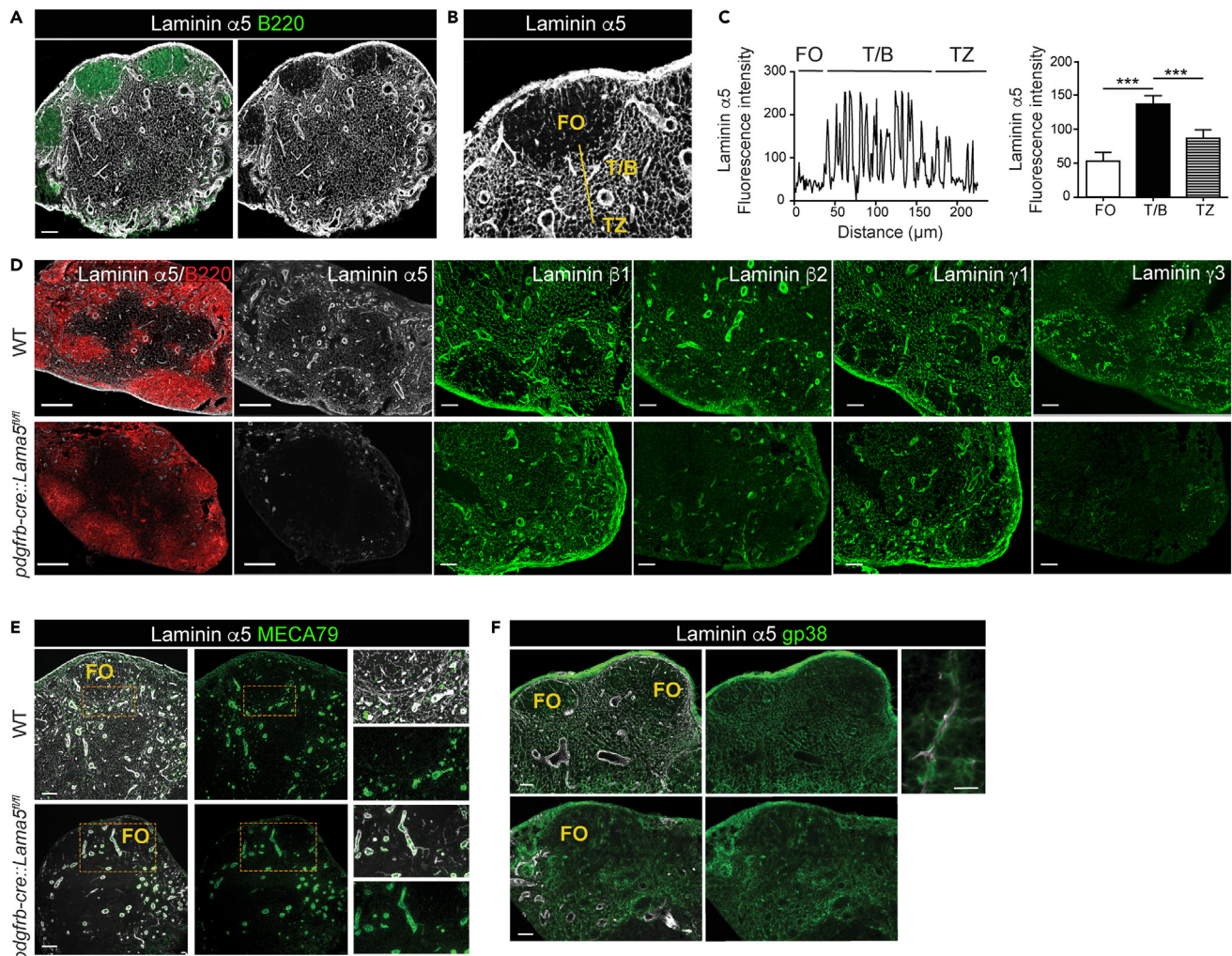
Figure 1. Immunofluorescence staining for ECM components and FRC markers in *pdgfrb-cre::Lama5*$^{fl/fl}$ and WT (*Lama5*$^{fl/fl}$) naive lymph nodes

(A–C) (A and B) Sections of WT adult lymph nodes were double stained for laminin α5 and B220; fluorescence intensities of laminin α5 staining from the follicle (FO) through the T-/B-cell border (T/B) to the T-cell zone (TZ) (yellow line in B) are shown in (C). Bar graph shows laminin α5 mean fluorescence intensities in FO, T/B and TZ measured in 20 sections from 4 WT and 4 *pdgfrb-cre::Lama5*$^{fl/fl}$ mice; data are means ± SD, analyzed using a Mann–Whitney U test; ***p <0.001.

(D) Double staining of WT and *pdgfrb-cre::Lama5*$^{fl/fl}$ lymph nodes for laminin α5 and B220; consecutive sections were stained for laminin β1, β2, γ1 and γ3 chains.

(E and F) (E) Double staining of WT and *pdgfrb-cre::Lama5*$^{fl/fl}$ lymph nodes for laminin α5 and MECA79 (PNAd) and (F) gp38 (podoplanin); boxed areas are shown at high magnifications to the right. Scale bars are 100 μm in (A), 50 μm in (D and E), and 30 μm in (F).

See also Figure S1.

nodes (Figure 2A); similar results were obtained with gating on ICOS$^+$CXCR5$^+$CD4$^+$ Tfh-cells (Figure S3A). A similar pattern of results was observed at day 28 after immunization (Figure 2A).

Measurements of the corresponding NP-specific serum IgG1 and IgM antibodies revealed significantly reduced levels, in particular of IgG1 antibodies, in the *pdgfrb-cre::Lama5*$^{fl/fl}$ mice (Figure 2B). This was associated with a reduced frequency of Fas$^+$GL-7$^+$ GC B-cells (Figure 2C). We also measured fewer IgG1$^+$ B-cells and CD138$^+$ plasma cells in the draining lymph nodes of immunized *pdgfrb-cre::Lama5*$^{fl/fl}$ mice compared to WT controls (Figures S3B and S3C). To exclude general defects in T and B cell development, we examined CD4$^+$ and CD8$^+$T-cells, B220$^+$ B-cells, CD11b$^+$ and CD11c$^+$ cells in the bone marrow and thymus of *pdgfrb-cre::Lama5*$^{fl/fl}$ mice and WT littermates, revealing no differences (Figures S4A and S4B). Taken together, the data suggest that GC form but that there are fewer GC B cells in mice lacking laminin α5 expression by reticular fibroblasts.
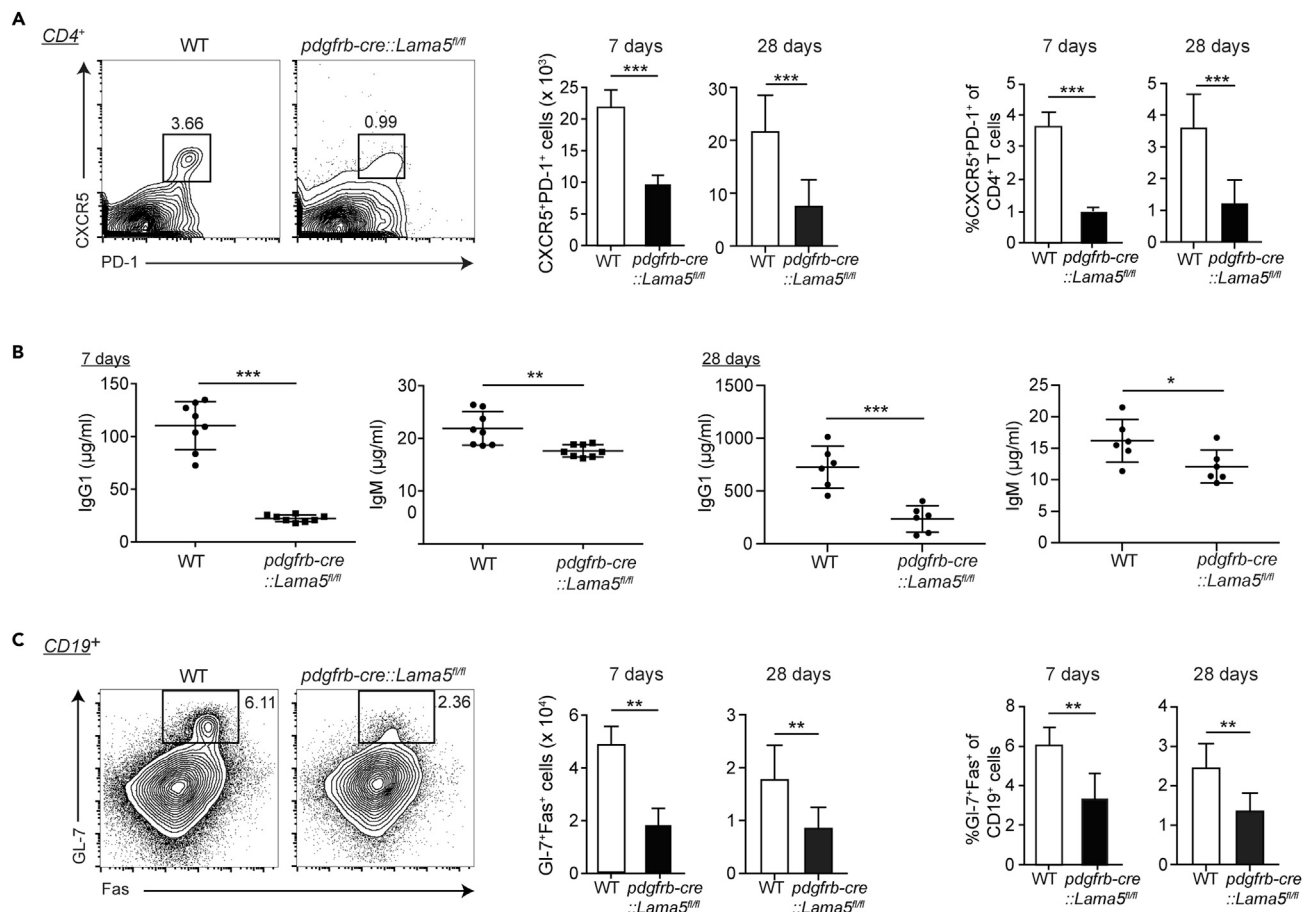
Figure 2. Immune response of *pdgfrb-cre::Lama5^{fl/fl}* and WT (*Lama5^{fl/fl}*) mice at days 7 and 28 after NP-CG immunization

(A–C) Lymph nodes were isolated at days 7 and 28 after immunization and analyzed by flow cytometry for (A) CD4⁺CXCR5⁺PD-1⁺ Tfh-cells; bar graphs show quantification of cell numbers and proportions; (B) corresponding serum antigen-specific IgG1 and IgM levels and (C) flow cytometry of CD19⁺Fas⁺GL-7⁺ GC B-cells; bar graphs show quantification. Flow cytometry in A and C are representative data. Graphs in A, B and C are means ± SD of 3 experiments performed with 7 WT and 7 *pdgfrb-cre::Lama5^{fl/fl}* mice. Data were analyzed using a Mann Whitney U test; **p <0.01; ***p <0.001. See also Figure S3.

Inter-relationship between the RF network at the B-cell follicle borders and antigen specific B- and pre-Tfh-cell populations

As the localization of Tfh- and B-cells is also important for GC formation, we transferred OVA-specific OTII-Tomato T-cells and NP-specific B1-8^{high}GFP B-cells into WT or *pdgfrb-cre::Lama5^{fl/fl}* recipients to track these cells *in vivo*. Mice were subsequently immunized the mice with NP-OVA and lymph nodes were analyzed after 36h. Analysis of total Tomato⁺ and GFP⁺ cells revealed similar numbers and proportions of donor cells in both recipients (Figure S5), indicating similar survival of donor cells in WT or *pdgfrb-cre::-Lama5^{fl/fl}* recipients. The localization of donor OTII-Tomato⁺T-cells and NP-specific B1-8^{high}GFP B-cells relative to B-cell follicles, identified with DAPI nuclei staining, were also examined (Figure 3A). In WT recipients, aggregates of the antigen specific B-cells occurred at the borders of the B-cell follicles and in inter-follicular regions, and donor OTII-Tomato⁺T-cells accumulated close to the B-cell follicles (Figure 3A), whereas in *pdgfrb-cre::Lama5^{fl/fl}* both donor OTII-Tomato⁺T-cells and donor B1-8^{high}-GFP B-cells were more broadly dispersed in the T-cell zone and follicles, respectively (Figure 3A). Stereological analyses were performed on 5 sections each from 4 WT and 4 *pdgfrb-cre::Lama5^{fl/fl}* mice to measure the distance of donor T- and B-cells from the follicle border, revealing broader dispersion of both cell types in *pdgfrb-cre::Lama5^{fl/fl}* hosts (Figure 3B).

Owing to low numbers at 36h after immunization, corresponding flow cytometry was performed at 72h, revealing significantly reduced numbers and proportions of donor OTII-Tomato⁺ cells but also of host Tomato^{neg} CXCR5⁺CD4⁺ Tfh-cells in *pdgfrb-cre::Lama5^{fl/fl}* lymph nodes compared to WT recipients
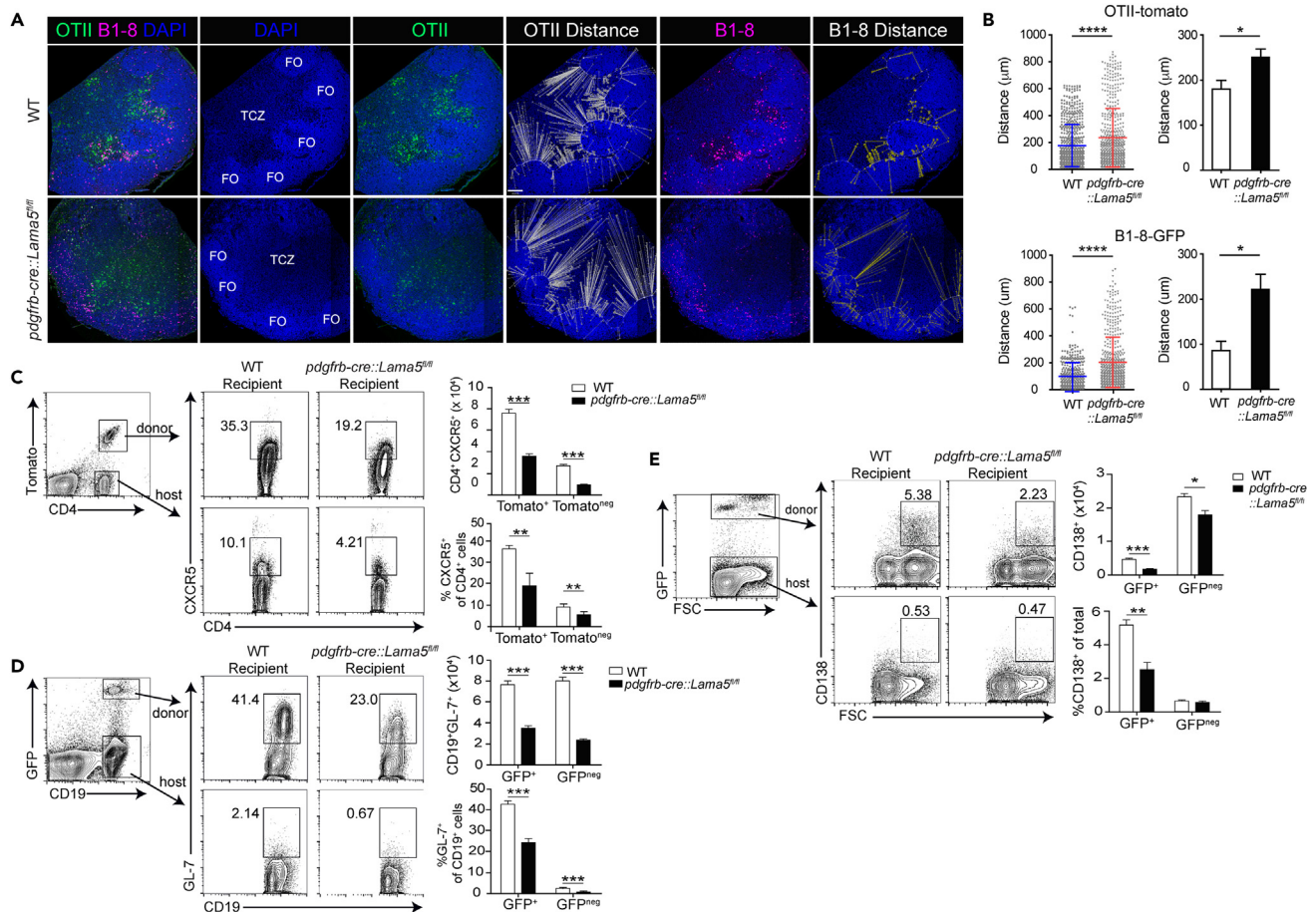
Figure 3. Inter-relationship between the RF network at the B-cell follicle borders and antigen specific B- and pre-Tfh-cell populations

(A) Representative immunofluorescence imaging for OVA-specific OTII-Tomato T-cells and NP-specific B1-8^{high}-GFPB-cells transferred into WT ($Lama5^{fl/fl}$) and $pdgfrb$-$cre::Lama5^{fl/fl}$ recipients; DAPI marks all cells and defines follicle borders; lymph nodes were analyzed at 36h after NP-OVA immunization.

(B–E) (B) Quantification of stereological analyses showing distances of OTII-tomato and B1-8^{high}-GFP cells from follicle borders (white and yellow lines, respectively, in (A)); data are means ± SD from 5 sections each from lymph nodes from 4 WT and 4 $pdgfrb$-$cre::Lama5^{fl/fl}$ mice. Flow cytometry at day 3 after transfer for (C) OTII-Tomato$^+$ and Tomato^{neg} CXCR5$^+$ pre-Tfh-cells, (D) B1-8-GFP$^+$ and B1-8-GFP^{neg} GL-7$^+$ GC cells and (E) CD19^{low} CD138$^+$ plasma cells in WT and $pdgfrb$-$cre::Lama5^{fl/fl}$ recipients; bar graphs show means and proportions ± SD of 3 experiments performed with 7 WT and 7 $pdgfrb$-$cre::Lama5^{fl/fl}$ recipients. Data were analyzed using a Mann Whitney U test; *p <0.05, **p <0.01, ***p <0.001; ****p <0.0001. See also Figure S3.

(Figure 3C). However, other T-cell subsets, such as the FoxP3$^+$ regulatory T-cells (Tregs), Th1- and Th2-cells were not altered (Figure S6). Similarly, flow cytometry revealed reduced donor B1-8-GFP$^+$ and host GFP^{neg}GL-7$^+$CD19$^+$ GC B-cells in $pdgfrb$-$cre::Lama5^{fl/fl}$ lymph nodes compared to WT recipients (Figure 3D) and correspondingly lower antigen specific GFP$^+$ and GFP^{neg}CD19^{low}CD138$^+$ plasma cells (Figure 3E).

DC populations in lymph nodes of naive and OVA immunized mice

Our previous studies suggested that laminin α5 containing isoforms support adhesion of immature DCs to the RF in lymph nodes, thereby, affecting their ability to take up soluble antigens.[3] As close interactions between CD4$^+$T-cells and DCs are required for Tfh-cell maturation,[6] we investigated whether the absence of laminin α5 in RF affected DC numbers, localization or function. Flow cytometry of naive lymph nodes from $pdgfrb$-$cre::Lama5^{fl/fl}$ and WT mice showed no differences in total CD11c$^+$ mature (CD11c$^+$MHC-II$^+$) or immature (CD11c$^+$MHCII^{neg}) DCs (Figure 4A). Similar results were obtained in WT and $pdgfrb$-$cre::Lama5^{fl/fl}$ mice after immunization with OVA$_{323-339}$ (Figure 4B).

A subset of DCs, CD11b$^+$CD4$^+$CD8^{neg} DCIR2$^+$ DCs, also known as cDC2s, are important for antigen presentation to CD4$^+$T-cells. Under the influence of 7α,25-dihyroxycholesterol (7α,25-OHC), produced by RFs
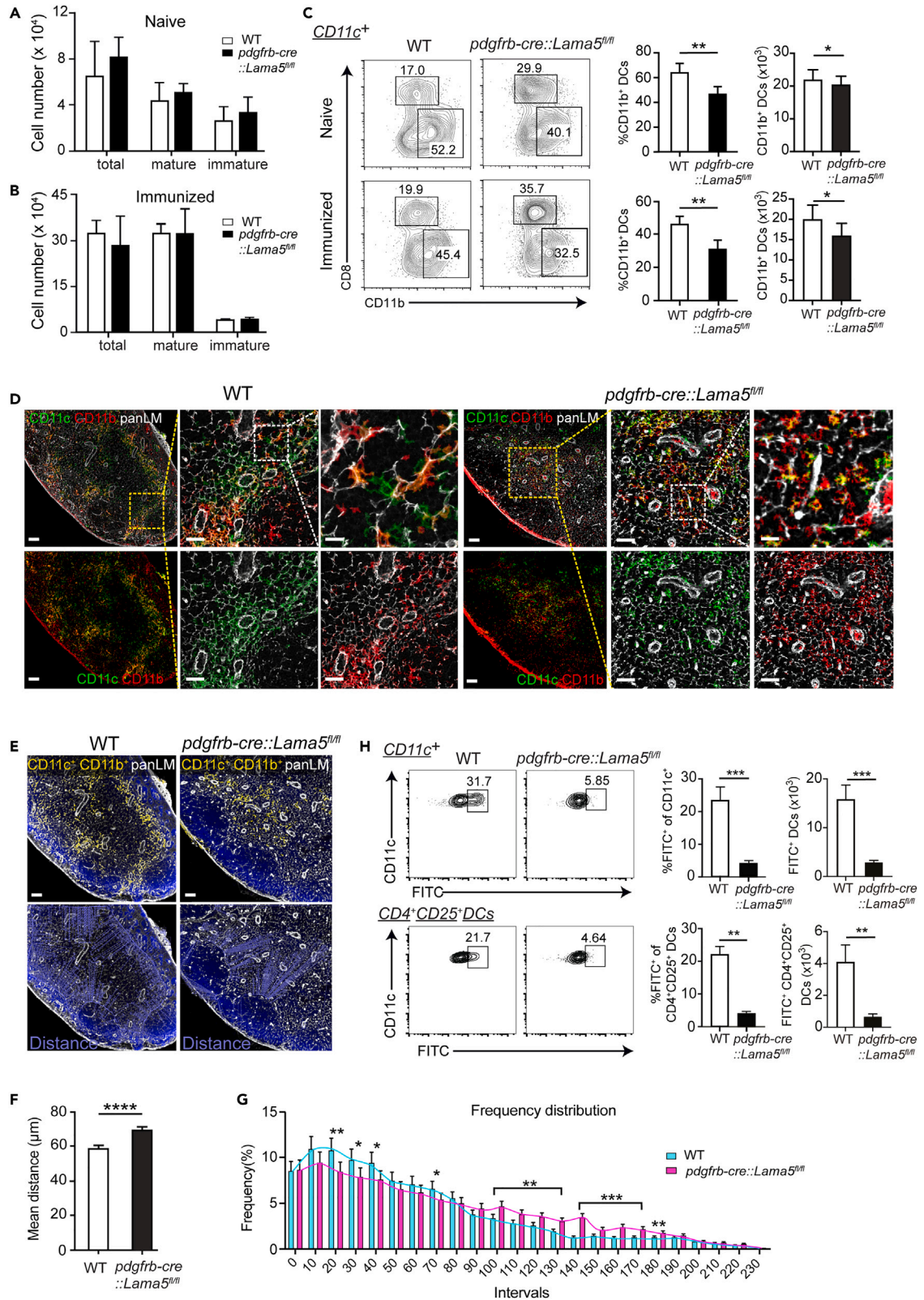
Figure 4. DC populations in lymph nodes of naive and OVA immunized *pdgfrb-cre::Lama5^fl/fl* and WT (*Lama5^fl/fl*) mice

(A–C) Flow cytometry of (A) total CD45$^+$CD11c$^+$ mature (MHC-II$^+$) and immature (MHCII^{neg}) DCs in naive and (B) OVA$_{323-339}$ immunized mice (at 1 week) and (C) corresponding flow cytometry for CD11c$^+$CD8^{neg}CD11b$^+$ DC numbers and proportions; data are means $\pm$ SD of 3 experiments with 5 *pdgfrb-cre::Lama5^fl/fl* and 3 WT controls.

(D) Immunofluorescence staining at 48h after immunization for CD11b$^+$CD11c$^+$ cDC2 and pan-laminin to mark RFs, boxed areas are shown at higher magnifications to the right; scale bars are 100 μm and 40 μm in high magnification images.

(E–G) (E) CD11b$^+$CD11c$^+$ double-positive cDC2 cells were pseudo-colored to illustrate their localization relative to the pan-laminin stained follicle borders; scale bars are 100μm; lower images show distances of individual cells from the follicle border employed for quantifications in (F) and (G); data in F and G are means $\pm$ SEM from 5 sections each from 4 WT and 4 *pdgfrb-cre::Lama5^fl/fl* lymph nodes.

(H) To address DC function, DQ-OVA was injected into the footpads of WT or *pdgfrb-cre::Lama5^fl/fl* mice and draining lymph nodes were analyzed at 2h by flow cytometry for numbers and proportions of CD11c$^+$FITC$^+$ DCs and FITC$^+$CD11c$^+$CD4$^+$CD25$^+$ DCs; bar graphs show means $\pm$ SD of 3 experiments with 7 WT and 7 *pdgfrb-cre::Lama5^fl/fl* mice. All data were analyzed using Mann Whitney U tests; *p <0.05; **p <0.01; ***p <0.001; ****p <0.0001.

at the follicle border, cDC2s localize to the follicle border where they have access to B-cell-derived lymphotoxin α1β2 which is required for their survival.[23] We therefore analyzed this population by flow cytometry in the steady state and 48h after immunization. In both cases, lower proportions of CD11b$^+$CD4$^+$CD8^{neg} cDC2s were measured in *pdgfrb-cre::Lama5^fl/fl* compared to WT lymph nodes, with a corresponding increase in the CD8$^+$CD11b$^+$ cDC1 population (Figure 4C).[24] Given that total DCs numbers do not change in *pdgfrb-cre::Lama5^fl/fl* lymph nodes, this suggests a change in the balance of cDC2 to cDC1s in *pdgfrb-cre::Lama5^fl/fl* lymph nodes.

Localization of cDC2s *in vivo* is difficult and although staining for DCIR2 has been reported,[25] we were not able to obtain reliable and reproducible staining. As cDC2s are CD11c$^+$ and CD11b^{high}[23,24] we employed these two markers in immunofluorescence staining to localize cDC2s *in vivo*. This revealed many CD11c$^+$ cells associated with laminin$^+$ RFs throughout the lymph node as we have previously reported[3] (Figure 4D), and concentration of the double-positive cells in close proximity to B-cell follicles (Figure 4D). In *pdgfrb-cre::Lama5^fl/fl* lymph nodes, fewer double-positive DCs associated with the laminin$^+$ RF around follicles compared to WT and they appeared further displaced toward the T-cell zone (Figure 4D). Stereological analyses performed on 5 sections each from 4 WT and 4 *pdgfrb-cre::Lama5^fl/fl* lymph nodes to measure the distance of the double-positive cDC2s from the follicle border revealed broader dispersion of these cells in the T-cell zone of *pdgfrb-cre::Lama5^fl/fl* lymph nodes (Figures 4E–4G). As cDC2s occur close to the follicle border, to more clearly illustrate the range of distances occupied by these cells we additionally calculated the frequency distribution of double-positive cells at defined distances from the follicle border. This revealed a second peak of cDC2s at larger distances from the follicle edge in *pdgfrb-cre::Lama5^fl/fl* lymph nodes which was not present in WT controls (Figure 4G).

Consequences of cDC2 dislocation

To investigate functional consequences of cDC2 interaction with RFs we employed footpad injections of fluorescently quenched ovalbumin (DQ-OVA),[3] immediately removed the draining lymph nodes and analyzed them by flow cytometry for FITC$^+$CD4$^+$CD25$^+$CD11c$^+$ cDC2s. This revealed reduced numbers of FITC$^+$ cDC2s in the lymph nodes of *pdgfrb-cre::Lama5^fl/fl* mice (Figure 4H), further substantiating displacement of the cDC2s from the RFs.

To test whether cDC2 survival/turnover was altered in *pdgfrb-cre::Lama5^fl/fl* lymph nodes we performed *in vivo* BrdU experiments followed by flow cytometry to quantify BrdU$^+$CD4$^+$CXCR5$^+$ Tfh-cells and BrdU$^+$CD4^{low}CXCR5^{neg}CD11c$^+$ cells that are likely to represent the cDC2s. These experiments revealed no statistically significant differences in the proportions of proliferating Tfh-cells and cDC2s, although there was a tendency toward higher proportions of BrdU$^+$ Tfh-cells in *pdgfrb-cre::Lama5^fl/fl* lymph nodes compared to WT controls (Figures S7A and S7B). Taken together, the data suggest that laminin α5 expression by FRCs contributes to cDC2 differentiation and localization at the B-cell follicle border but not to their survival, and that cDC2 interactions with pre-Tfh-cells are compromised in the absence of laminin α5.

To further investigate defects in interactions between cDC2s and pre-Tfh-cells, we investigated events downstream of these interactions. As cDC2s bind large amounts of IL-2, reduction or displacement of this population from the B-cell follicle border would result in excessive IL-2 signaling in the pre-Tfh-cells and, thereby, higher levels of phosphorylated Stat5.[26] p-Stat5 levels were, therefore, measured in CD4$^+$CXCR5$^+$ pre-Tfh-cells on day 3 after immunization, revealing significantly higher levels in pre-Tfh-cells from *pdgfrb-cre::Lama5^fl/fl* lymph nodes (Figure 5A). ICOS-ICOSL interactions are also required for Tfh-cell
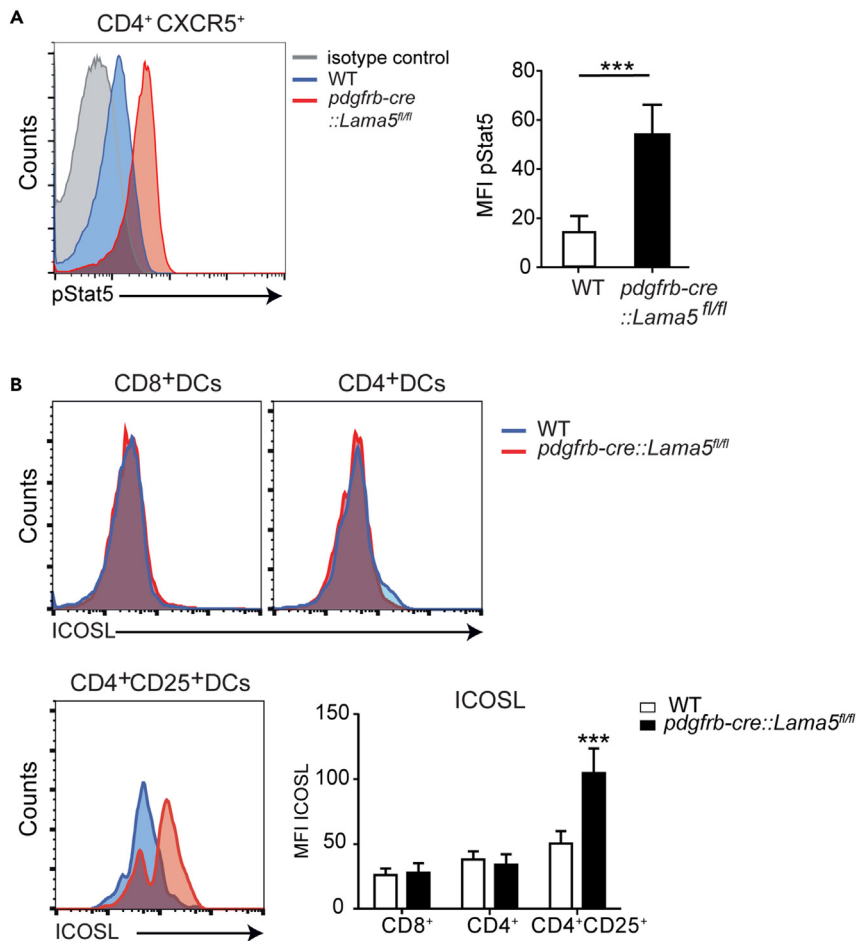
Figure 5. Consequence of cDC2 dislocation

(A and B) (A) Intracellular MFI of p-STAT5 in Tfh-cells, and (B) ICOSL on the surface of CD11c$^+$CD8$^+$ DCs, CD11c$^+$CD4$^+$ DCs and CD11b$^+$CD11c$^+$CD4$^+$CD25$^+$ cDC2s. Bar graphs are means $\pm$ SD of 3 experiments performed with 6 WT and 6 *pdgfrb-cre::Lama5*$^{fl/fl}$ mice. All data were analyzed using Mann Whitney U tests; ***p <0.001.

differentiation and ICOSL is shed from the DC surface subsequent to interaction with Tfh-cells. Hence, DC shedding of ICOSL[27,28] can be used as an indirect measure of interactions between DCs and pre-Tfh-cells.[29] We, therefore, analyzed CD11c$^+$CD4$^+$CD25$^+$ICOSL$^+$ DCs after immunization with OVA$_{323-339}$. Two peaks of ICOSL expression were measured in CD4$^+$CD25$^+$ DCs in *pdgfrb-cre::Lama5*$^{fl/fl}$ mice – a larger, high concentration and a smaller, low concentration peak – compared to only the lower concentration peak in WT mice (Figure 5B). This suggests that most CD4$^+$CD25$^+$ DCs do not shed ICOSL in *pdgfrb-cre::Lama5*$^{fl/fl}$ mice, consistent with fewer interactions with pre-Tfh-cells.

cDC2 interact with laminin α5 of RFs via integrin α6β1

Our data suggest reduced differentiation and dislocation of cDC2s in *pdgfrb-cre::Lama5*$^{fl/fl}$ lymph nodes which may be due to laminin α5 effects on FRCs or direct binding of cDC2s to the laminin layer of the RF, which we have previously demonstrated can occur.[3] Higher magnification analyses of the CD11b$^+$CD11c$^+$ cDC2s on RFs in the *pdgfrb-cre::Lama5*$^{fl/fl}$ lymph nodes revealed that the cells were smaller and less spread than in the WT lymph nodes (Figure 4D), consistent with a direct interaction of cDC2s with laminin α5 in the RFs. To test this possibility, we investigated by flow cytometry whether cDC2s express laminin binding integrins, revealing expression of integrins α6β1, αvβ1 and/or αvβ3 (Figure S8), all of which can bind to the laminin α5 chain but recognize different domains on the molecule.[30,31] Due to its limited distribution *in vivo*, laminin 523 cannot be purified from tissues and is not available as a recombinant protein. We, therefore, performed *in vitro* adhesion assays using laminin 511/521,
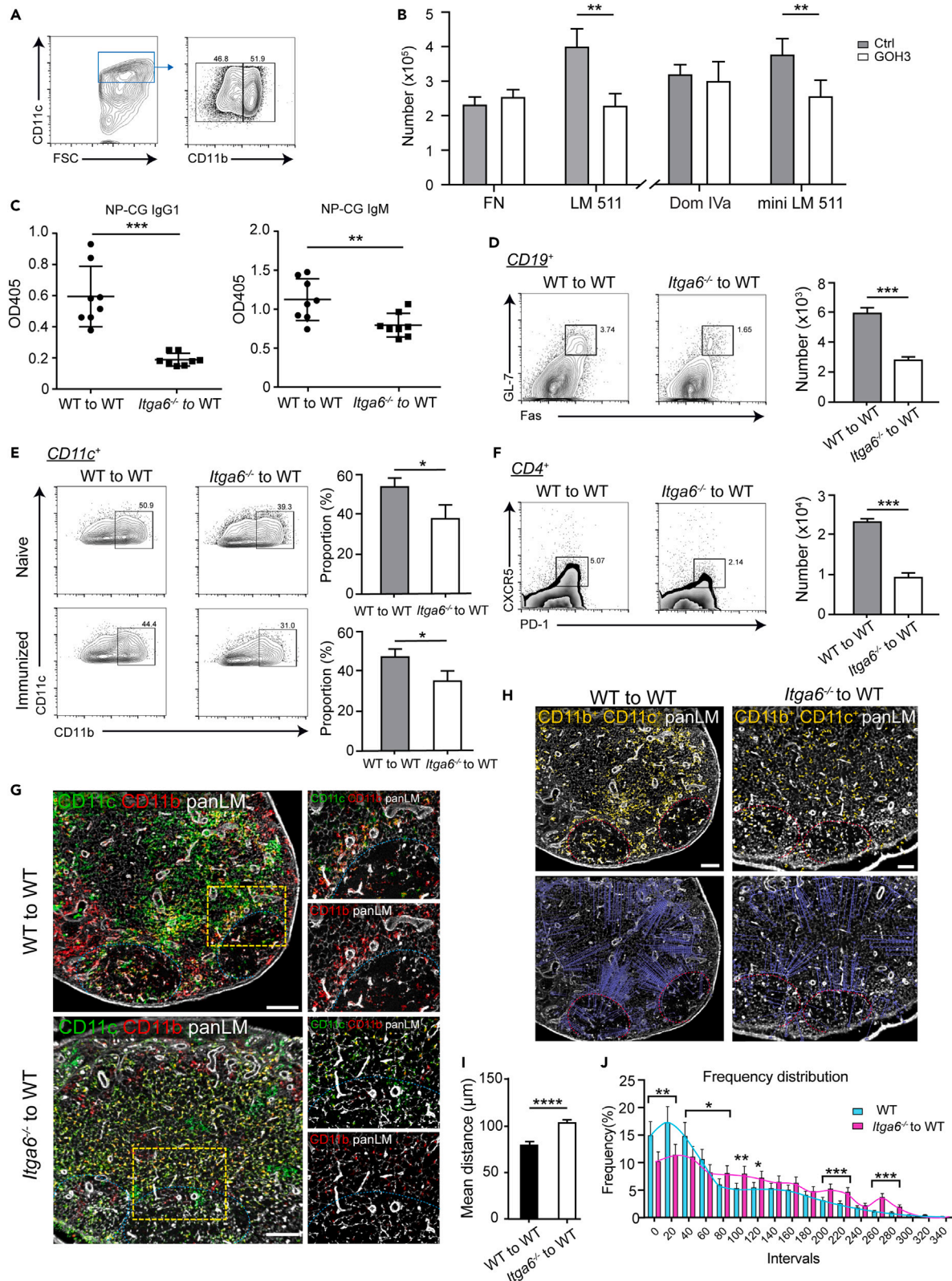
Figure 6. cDC2 interact with laminin α5 of RFs via integrin α6β1

(A–F) (A) Gatings employed to analyze CD11c⁺CD11b⁺ cDC2s (B) bound to laminin 511 and specific domains thereof, or fibronectin (FN) control, in the presence of function blocking integrin α6β1 antibody (GoH3); data are means ± SD of 3 experiments with triplicates in each experiment and analyzed by Student's *t* test; **p <0.01. Lymph nodes from WT hosts carrying *Itga6*⁻ᐟ⁻ or WT bone marrow were isolated 1 week after immunization and analyzed by flow cytometry for (C) antigen specific IgG1 and IgM levels, (D) CD19⁺Fas⁺GL-7⁺ GC B-cells, (E) CD11b⁺CD11c⁺ cDC2, (F) CD4⁺CXCR5⁺PD-1⁺ Tfh-cells; bar graphs show means ± SD from 3 WT and 3 *Itga6*⁻ᐟ⁻ chimerics; data were analyzed by Student's *t* test; *p<0.05, **p<0.01; ***p<0.001.

(G) Immunofluorescence staining at 48h after immunization for CD11b⁺CD11c⁺ cDC2 and pan-laminin to mark RFs in WT and *Itga6*⁻ᐟ⁻ chimeras; scale bars are 150 μm.

(H–J) (H) CD11b⁺CD11c⁺ double-positive cDC2s were pseudo-colored to illustrate their localization relative to the pan-laminin stained follicle borders and RFs, scale bars are 100 μm in WT and 50 μm in *Itga6*⁻ᐟ⁻ chimeras; distances of individual cells from the follicle border were employed for quantifications in (I) and (J); data in I and J are means ± SEM from 5 sections each from 4 WT and 4 *Itga6*⁻ᐟ⁻ lymph nodes. Data were analyzed using a Mann Whitney U test; ****p <0.0001.

See also Figures S4 and S5.

recombinant laminin α5 domain IVa which engages αv integrins, and the C-terminal domain of laminin 511 (mini LM511) recognized by integrin α6β1; fibronectin which we have previously shown to be an adhesive substrate for CD11c⁺ cells[3] was employed as a control substrate. Total CD11c⁺ cells were isolated from lymph nodes, allowed to bind to the substrates for 90 min at 37°C and bound CD11c⁺CD11b⁺ cDC2s were quantified by flow cytometry (Figure 6A). This revealed significant binding of cDC2s to fibronectin, laminin 511/521, laminin α5 domain IVa and mini LM511 and inhibition of binding only to laminin 511/521 and mini LM511 by a functional blocking integrin α6β1 antibody (Figure 6B). Adhesion was not completely ablated suggesting the involvement of another integrin, potentially αvβ1/αvβ3,[31] which is suggested by the binding of CD11c⁺CD11b⁺ cells to domain IVa of laminin α5 (Figure 6B).

To investigate a direct role for integrin α6β1-mediated adhesion to RF laminin α5 in cDC2 location and function *in vivo*, we generated bone chimeric mice carry *Itga6*⁻ᐟ⁻ or WT bone marrow in WT hosts. Staining for pan laminin revealed no overt differences in lymph node morphology or follicle numbers, nor defects in follicle borders (Figures 6G and 6H). Chimeras were immunized with the T-cell dependent antigen NP-CGG and after one week antibody titers were determined. This revealed lower circulating levels of IgG and IgM specific antibodies in the *Itga6*⁻ᐟ⁻ chimeras (Figure 6C) and reduced numbers of GC B-cells (Figure 6D), cDC2s (Figure 6E) and Tfh-cells (Figure 6F) in lymph nodes, as observed in *pdgfrb-cre::Lama5^fl/fl^* mice, albeit with less extensive effects. Localization of cDC2s as defined by double CD11c/CD11b staining together with pan-laminin staining to identify RFs, revealed displacement of cDC2s toward the T-cell zone in lymph nodes of *Itga6*⁻ᐟ⁻ chimeras (Figure 6G). Stereology confirmed larger distances between CD11b⁺CD11c⁺ cDC2s and follicle borders in lymph nodes of the *Itga6*⁻ᐟ⁻ chimeras (Figures 6H–6J).

cDC2 uptake of DQ-OVA after footpad injection was also reduced in the *Itga6*⁻ᐟ⁻ chimeras (Figure S9). Although the effects observed were not as extensive as in *pdgfrb-cre::Lama5^fl/fl^* mice, these results support the possibility of direct binding of cDC2s to laminin α5 of RFs via integrin α6β1, and potentially another αv integrin, and that this contributes to their localization.

Characterization of FRC phenotypes in lymph nodes

As FRCs express different markers at different sites in the lymph nodes and ensheath the outer basement membrane layer of RFs, we also investigated potential changes in FRCs in the *pdgfrb-cre::Lama5^fl/fl^* mice. 7α,25-dihyroxycholesterol (7α,25-OHC) secretion by FRCs at the follicle border is critical for localization of CD4⁺ DCs, pre-Tfh-cells and B-cells to this site; we therefore investigated the expression of the enzymes, Cyp7b1 and Ch25h, required for its synthesis.[15] According to a recent scRNA-Seq study, these enzymes are expressed primarily by PDGFrecβ⁺CCL19^low^ FRCs at the T-/B-cell border.[13] Our data (Figure 1F) and that of others[22] indicate that this population is also podoplanin/gp38^low^ (Figures S10A–S10C).[13,32] We, therefore, employed flow cytometry to sort the CD45⁺CD31^neg^PDGFrecβ⁺gp38 high and low FRC populations from lymph nodes of naive and day 3 immunized *pdgfrb-cre::Lama5^fl/fl^* mice and their WT littermates, and analyzed them by qPCR for the expression of *Cyp7b1* and *Ch25h* as well as other genes known to be differentially expressed in CCL19^low^ FRCs.[13]

Numbers of CD45⁺CD31^neg^PDGFrecβ⁺gp38 high and low FRC populations from lymph nodes of *pdgfrb-cre::Lama5^fl/fl^* mice and their WT littermates did not differ. However, qPCR confirmed the almost exclusive expression of *Ch25h* by the PDGFrecβ⁺CCL19^low^gp38^low^ FRCs (Figure 7A) and revealed significantly reduced expression of *Cyp7b1* and *Ch25h* in this population of FRCs in *pdgfrb-cre::Lama5^fl/fl^* mice
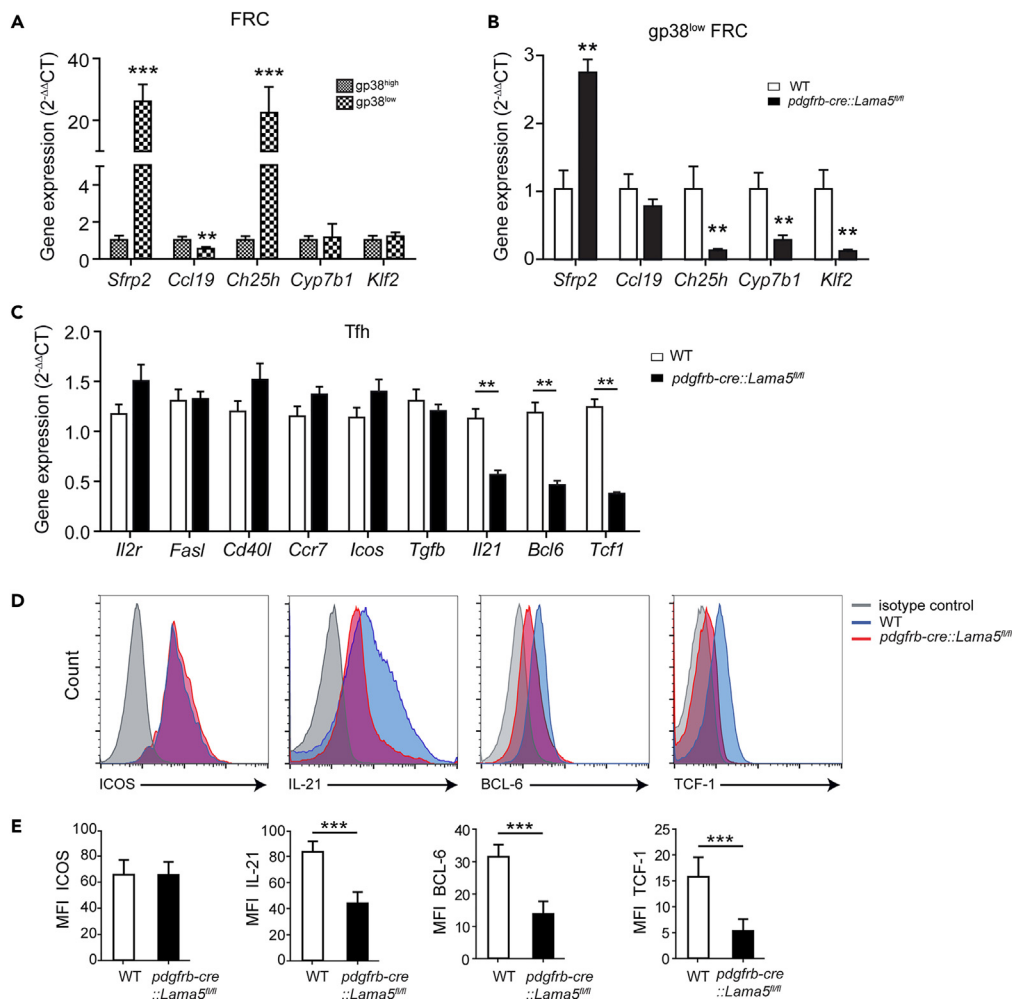
Figure 7. Characterization of FRC phenotypes in lymph nodes of *pdgfrb-cre::Lama5^{fl/fl}* and WT (*Lama5^{fl/fl}*) mice immunized with OVA and analyzed at 1 week after immunization

(A) FRCs were sorted from lymph nodes of WT mice and CD45$^+$CD31^{neg}PDGFrecβ$^+$gp38 high and low populations were analyzed by qPCR for markers of follicle border specific FRCs;

(B) the same analyses were performed on sorted CD45$^+$CD31^{neg} PDGFrecβ$^+$gp38^{low} FRCs from OVA immunized *pdgfrb-cre::Lama5^{fl/fl}* mice and WT controls. Data in A and B are expressed as relative fold difference and are means $\pm$ SD of 2 experiments performed with 8 *pdgfrb-cre::Lama5^{fl/fl}* and 6 WT mice. Data were analyzed using a Mann Whitney U test, **p <0.01; ***p <0.001.

(C–E) (C) Sorted CD4$^+$PD-1$^+$CXCR5$^+$ Tfh-cells from *pdgfrb-cre::Lama5^{fl/fl}* and WT lymph nodes were analyzed by qPCR and (D) results were verified by flow cytometry of CD4$^+$T-cells and quantified in (E). Mean fluorescence intensity (MFI) in (E) are means $\pm$ SD of 4 experiments performed with 4 *pdgfrb-cre::Lama5^{fl/fl}* and 4 WT mice. Data were analyzed by Mann Whitney U tests; ***p <0.001.

See also Figure S6.

(Figure 7B). Accordingly, RNA Scope for C*h25h* at day 7 after immunization further revealed a lower signal in the lymph nodes of *pdgfrb-cre::Lama5^{fl/fl}* mice compared to WT littermates and less association with follicle borders (Figure S10D). Of interest, other factors previously shown to be specifically expressed by the PDGFrecβ$^+$CCL19^{low}gp38^{low} FRCs (Figures S10A–S10C) were also altered in *pdgfrb-cre::Lama5^{fl/fl}* (Figure 7B).[13] One such molecule was secreted frizzled-related protein 2 (*Sfrp2*) (Figures 7A and 7B), a soluble modulator of Wnt signaling that sequesters free Wnts and, hence, competes with Wnt binding to frizzled receptors.[33] Wnt signaling induces β-catenin nuclear translocation which competes with a T-cell factor (TCF) repressor protein, leading to enhanced transcriptional activity of TCF-1 required for BCL-6 expression and Tfh cell commitment.[17,18] We, therefore, performed qPCR on sorted CD4$^+$PD-1$^+$CXCR5$^+$ Tfh-cells from *pdgfrb-cre::Lama5^{fl/fl}* and WT lymph nodes after OVA$_{323-339}$ immunization, revealing significantly

reduced expression of *Tcf1*, *Il21* and *Bcl6* in Tfh-cells from *pdgfrb-cre::Lama5^{fl/fl}* mice (Figure 7C), consistent with the reduced Tfh differentiation and GC B-cells observed in these mice; these results were confirmed at the protein level (Figures 7D and 7E).

DISCUSSION

Stromal FRCs surrounding B-cell follicles have been shown to be a specialized subpopulation of FRCs, responsible for optimizing the GC reaction.[13,32] The data presented here indicates that the ECM composition of RFs, specifically laminin 523, at this site also contributes to the unique molecular signature of these FRCs and, in addition, affects differentiation of cDC2s and their localization at the follicle border, both required for pre-Tfh-cell activation.

We observed that laminin α5-deficient FRCs fail to adequately support Tfh differentiation and subsequently also GC B-cell formation. We provide evidence that laminin α5 critically promotes expression of enzymes required for production of 7α,25OHC at the T-/B-cell border and, thereby, influences the localization of pre-Tfh-cells, B-cells and cDC2s at this site. In addition, laminin 523 affects the differentiation of the cDC2s within the lymph node, potentially by integrin-mediate interaction of incoming DCs with laminin α5 in the RF.

The ECM of the RFs at the border of the B-cell follicle was found to be unique in its composition, containing not only laminin α5 but also laminin β2 and γ3 chains to form laminin 523, a rare isoform with limited distribution to selective blood vessel basement membranes of the retina and brain and some epithelial basement membranes.[21] By contrast, the RFs of the T-cell zone expressed laminin α5, β1 and γ1 chains, suggesting the occurrence of the more broadly distributed laminin 511 isoform.[20] As FRCs are considered to secrete their specialized ECM core, this supports the concept that FRCs are a heterogeneous group of cells with different functions depending on their location, as suggested also by others.[13,32] Although FRCs increase in size and number under inflammatory conditions,[34,35] recent scRNA-Seq data from *in vivo* isolated FRCs suggest that there is low turn-over, if any, of the core ECM constituents of the RFs, i.e., laminins and collagen types IV and I/III.[13] Rather, microfibrillar proteins of the RFs that act to connect the inner fibrillar collagen core to the ensheathing basement membrane layer, such as fibrillins, SPARC (BM40) and collagen VI, are differentially expressed in inflammation versus homeostatic conditions.[36] This suggests minimal remodeling, such that movement of the fibrillar collagen core relative to the outer BM layer is promoted, permitting expansion and rapid return to normal lymph node dimensions as occurs in inflammation, without overt changes in the RF network scaffold. It may be, therefore, that the major fibrillar collagens and, in particular, the outer BM proteins of RFs represent a type of tissue memory, guiding the differentiation and also localization of newly formed FRCs but also DCs migrating into the lymph node in inflammatory conditions.

Laminin α5 was shown here to promote expression of *Ch25h* by the PDGFrecβ⁺CCL19^{low}gp38^{low} FRCs located at the border to the B-cell follicles, required for 7α,25-OHC production and, thereby, the attraction of B-cells, pre-Tfh-cells and CD4⁺CD25⁺ DCs to this site.[15] Given the close association between FRCs and the underlying BM component of the RFs this is probably mediated by direct interactions. This is substantiated by the expression of integrin α6β1 by FRCs,[3,13] which can bind to laminin α5 containing isoforms.[3,13] Although T-cells can also bind to laminin α5 containing isoforms,[30,37] data from different sources[3,36,38] suggest that the BM layer of the RF is not exposed to permit adhesion of T-cells. Rather, T-cells interact with and migrate on the FRCs, and can also affect FRC biology.[39,40] By contrast, immature DCs interdigitate with FRCs along the fiber length and have been shown to bind to RF laminins and to take up soluble antigen/substances from the core of RFs.[3] Although our *in vitro* adhesion assays were performed with laminin 511, as laminin 523 cannot be isolated for such experiments, the adhesion of cDC2s to this laminin α5-containing isoform, together with the reduction in the cDC2 numbers observed in the *pdgfrb-cre::Lama5^{fl/fl}* mice, suggests that the interaction of DCs migrating into the lymph node with laminin 523 may promote the differentiation of this population. Although indirect evidence, the similar phenotype of the *Itga6^{−/−}* bone marrow chimeras and the *pdgfrb-cre::Lama5^{fl/fl}* mice, substantiates this possibility. Furthermore, laminin 523 modulation of the FRC phenotype and expression of factors such as Wnts, which may also affect DC sub-populations,[41] cannot be excluded. This is supported by the fact that TCF-1/LEF is also expressed by DCs[42–44] and by studies showing a role for Wnt signaling in DC maturation.[41,45]

The upregulated expression of *Sfrp2* in PDGFrecβ⁺gp38^{low} perifollicular FRCs of *pdgfrb-cre::Lama5^{fl/fl}* lymph nodes (30-fold increase) may suggest a role for laminin α5 in modulating Wnt signaling in FRCs.

This can directly affect Tfh-cell differentiation by induction of *Tcf-1* and *Bcl-6* expression, as shown here, but as mentioned above could also affect development of the $CD4^+CD25^+DCIR2^+$ cDC2 population. sFRP-2 binds several Wnts and, thereby, acts as an antagonist to Wnt binding to frizzled receptors.[46] It belongs to a family of 8 members that, together with Wnt inhibitory factor (WIF)-1 and the Dickkopf (DDK) family, act to regulate functions of Wnts involved in both canonical and non-canonical signaling pathways. Although sFRPs are secreted, several reports indicate that sFRPs synthesized by cultured cells are found mainly at the plasma membrane or in the ECM. As heparin treatment of cultured cells releases FRPs into the culture medium, it is thought that sFRP association with heparan sulfate proteoglycans either on the cell surface or in the ECM stabilizes Wnt-sFRP complexes or determines antagonist localization.[46] Unfortunately, it is not possible to stain for Wnts *in situ*; however, re-analysis of published scRNA-seq data from lymph node FRCs revealed expression of Wnt5a in the $pg38^+CCL19^{low}$ FRC population.[13]

In conclusion, the effects of loss of laminin α5 expression by reticular fibroblasts are 2-fold - on the location and maintenance of the cDC2s at the follicle border but also on positioning of Tfh- and B-cells through reduced 7α,25-dihydroxycholesterol synthesis. Our data suggest that the basement membrane components of RFs, which are long-lived structures in the lymph node, represent a type of tissue memory, guiding the differentiation and localization of specialize FRC and DC populations at the follicle border, required for normal lymph node function.

Limitations of the study

Difficulty in identification of the cDC2 population and *in vivo* targeting of specific ECM adhesion receptors on this population is one limitation that prevents definitive proof that these cells interact with laminin α5 at the follicle border, that the specific laminin isoform is laminin 523, and that this influences their differentiation into cDC2s. The same is true for the follicle bordering reticular fibroblasts.

STAR★METHODS

Detailed methods are provided in the online version of this paper and include the following:

- KEY RESOURCES TABLE
- RESOURCE AVAILABILITY
  - Lead contact
  - Materials availability
  - Data and code availability
- EXPERIMENTAL MODEL AND SUBJECT DETAILS
- METHOD DETAILS
  - Immunization/antibody response
  - Adoptive transfer
  - Immunofluorescence
  - Flow cytometry
  - Antibodies employed
  - DC cell adhesion assay
  - BrdU incorporation
  - FRC and Tfh-cell sorting and qPCR analyses
  - scRNA analysis
  - RNAscope
- QUANTIFICATION AND STATISTICAL ANALYSIS

SUPPLEMENTAL INFORMATION

Supplemental information can be found online at https://doi.org/10.1016/j.isci.2023.106753.

AUTHOR CONTRIBUTIONS

J.S. performed most experiments and together with L.S. designed experiments. L.S. provided funding for the project and infrastructure, and wrote the manuscript; S.C. and N.L. provided guidance and tools for analyses of B-cells and contributed to manuscript compilation; TP contributed to re-analysis of published scRNA-Seq data; XZ contributed to the OTII-tomato+T-cells and B1-8-GFP B-cell transfer experiments; M.H. contributed to data analyses and presentation.

DECLARATION OF INTERESTS

The authors declare no competing interests.

INCLUSION AND DIVERSITY

We support inclusive, diverse, and equitable conduct of research.

REFERENCES

1. De Silva, N.S., and Klein, U. (2015). Dynamics of B cells in germinal centres. Nat. Rev. Immunol. *15*, 137–148. https://doi.org/10.1038/nri3804.

2. Song, J., Lokmic, Z., Lämmermann, T., Rolf, J., Wu, C., Zhang, X., Hallmann, R., Hannocks, M.J., Horn, N., Ruegg, M.A., et al. (2013). Extracellular matrix of secondary lymphoid organs impacts on B-cell fate and survival. Proc. Natl. Acad. Sci. USA *110*, E2915–E2924. https://doi.org/10.1073/pnas.1218131110.

3. Sixt, M., Kanazawa, N., Selg, M., Samson, T., Roos, G., Reinhardt, D.P., Pabst, R., Lutz, M.B., and Sorokin, L. (2005). The conduit system transports soluble antigens from the afferent lymph to resident dendritic cells in the T cell area of the lymph node. Immunity *22*, 19–29.

4. Kerfoot, S.M., Yaari, G., Patel, J.R., Johnson, K.L., Gonzalez, D.G., Kleinstein, S.H., and Haberman, A.M. (2011). Germinal center B cell and T follicular helper cell development initiates in the interfollicular zone. Immunity *34*, 947–960. https://doi.org/10.1016/j.immuni.2011.03.024.

5. Lee, S.K., Rigby, R.J., Zotos, D., Tsai, L.M., Kawamoto, S., Marshall, J.L., Ramiscal, R.R., Chan, T.D., Gatto, D., Brink, R., et al. (2011). B cell priming for extrafollicular antibody responses requires Bcl-6 expression by T cells. J. Exp. Med. *208*, 1377–1388. https://doi.org/10.1084/jem.20102065.

6. Vinuesa, C.G., and Cook, M.C. (2011). Blood relatives of follicular helper T cells. Immunity *34*, 10–12. https://doi.org/10.1016/j.immuni.2011.01.006.

7. Weber, J.P., Fuhrmann, F., Feist, R.K., Lahmann, A., Al Baz, M.S., Gentz, L.J., Vu Van, D., Mages, H.W., Haftmann, C., Riedel, R., et al. (2015). ICOS maintains the T follicular helper cell phenotype by down-regulating Kruppel-like factor 2. J. Exp. Med. *212*, 217–233. https://doi.org/10.1084/jem.20141432.

8. Xu, H., Li, X., Liu, D., Li, J., Zhang, X., Chen, X., Hou, S., Peng, L., Xu, C., Liu, W., et al. (2013). Follicular T-helper cell recruitment governed by bystander B cells and ICOS-driven motility. Nature *496*, 523–527. https://doi.org/10.1038/nature12058.

9. Lu, E., and Cyster, J.G. (2019). G-protein coupled receptors and ligands that organize humoral immune responses. Immunol. Rev. *289*, 158–172. https://doi.org/10.1111/imr.12743.

10. Lokmic, Z., Lämmermann, T., Sixt, M., Cardell, S., Hallmann, R., and Sorokin, L. (2008). The extracellular matrix of the spleen as a potential organizer of immune cell compartments. Semin.Immunol. *20*, 4–13.

11. Bajénoff, M., Egen, J.G., Koo, L.Y., Laugier, J.P., Brau, F., Glaichenhaus, N., and Germain, R.N. (2006). Stromal cell networks regulate lymphocyte entry, migration, and territoriality in lymph nodes. Immunity *25*, 989–1001. https://doi.org/10.1016/j.immuni.2006.10.011.

12. Gerner, M.Y., Torabi-Parizi, P., and Germain, R.N. (2015). Strategically localized dendritic cells promote rapid T cell responses to lymph-borne particulate antigens. Immunity *42*, 172–185. https://doi.org/10.1016/j.immuni.2014.12.024.

13. Rodda, L.B., Lu, E., Bennett, M.L., Sokol, C.L., Wang, X., Luther, S.A., Barres, B.A., Luster, A.D., Ye, C.J., and Cyster, J.G. (2018). Single-cell RNA sequencing of lymph node stromal cells reveals niche-associated heterogeneity. Immunity *48*, 1014–1028.e6. https://doi.org/10.1016/j.immuni.2018.04.006.

14. Gretz, J.E., Norbury, C.C., Anderson, A.O., Proudfoot, A.E., and Shaw, S. (2000). Lymph-borne chemokines and other low molecular weight molecules reach high endothelial venules via specialized conduits while a functional barrier limits access to the lymphocyte microenvironments in lymph node cortex. J. Exp. Med. *192*, 1425–1440.

15. Yi, T., Wang, X., Kelly, L.M., An, J., Xu, Y., Sailer, A.W., Gustafsson, J.A., Russell, D.W., and Cyster, J.G. (2012). Oxysterol gradient generation by lymphoid stromal cells guides activated B cell movement during humoral responses. Immunity *37*, 535–548. https://doi.org/10.1016/j.immuni.2012.06.015.

16. Gatto, D., Wood, K., Caminschi, I., Murphy-Durland, D., Schofield, P., Christ, D., Karupiah, G., and Brink, R. (2013). The chemotactic receptor EBI2 regulates the homeostasis, localization and immunological function of splenic dendritic cells. Nat. Immunol. *14*, 446–453. https://doi.org/10.1038/ni.2555.

17. Xu, L., Cao, Y., Xie, Z., Huang, Q., Bai, Q., Yang, X., He, R., Hao, Y., Wang, H., Zhao, T., et al. (2015). The transcription factor TCF-1 initiates the differentiation of T(FH) cells during acute viral infection. Nat. Immunol. *16*, 991–999. https://doi.org/10.1038/ni.3229.

18. Choi, Y.S., Gullicksrud, J.A., Xing, S., Zeng, Z., Shan, Q., Li, F., Love, P.E., Peng, W., Xue, H.H., and Crotty, S. (2015). LEF-1 and TCF-1 orchestrate T(FH) differentiation by regulating differentiation circuits upstream of the transcriptional repressor Bcl6. Nat. Immunol. *16*, 980–990. https://doi.org/10.1038/ni.3226.

19. Xue, H.H., and Zhao, D.M. (2012). Regulation of mature T cell responses by the Wnt signaling pathway. Ann. N. Y. Acad. Sci. *1247*, 16–33. https://doi.org/10.1111/j.1749-6632.2011.06302.x.

20. Sorokin, L.M., Pausch, F., Frieser, M., Kröger, S., Ohage, E., and Deutzmann, R. (1997). Developmental regulation of the laminin alpha5 chain suggests a role in epithelial and endothelial cell maturation. Dev. Biol. *189*, 285–300.

21. Li, Y.N., Radner, S., French, M.M., Pinzón-Duarte, G., Daly, G.H., Burgeson, R.E., Koch, M., and Brunken, W.J. (2012). The gamma3

chain of laminin is widely but differentially expressed in murine basement membranes: expression and functional studies. Matrix Biol. *31*, 120–134. https://doi.org/10.1016/j.matbio.2011.12.002.

22. Novkovic, M., Onder, L., Cupovic, J., Abe, J., Bomze, D., Cremasco, V., Scandella, E., Stein, J.V., Bocharov, G., Turley, S.J., and Ludewig, B. (2016). Topological small-world organization of the fibroblastic reticular cell network determines lymph node functionality. PLoS Biol. *14*, e1002515. https://doi.org/10.1371/journal.pbio.1002515.

23. Lu, E., Dang, E.V., McDonald, J.G., and Cyster, J.G. (2017). Distinct oxysterol requirements for positioning naive and activated dendritic cells in the spleen. Sci. Immunol. *2*, eaal5237. https://doi.org/10.1126/sciimmunol.aal5237.

24. Cabeza-Cabrerizo, M., Cardoso, A., Minutti, C.M., Pereira da Costa, M., and Reis e Sousa, C. (2021). Dendritic cells revisited. Annu. Rev. Immunol. *39*, 131–166. https://doi.org/10.1146/annurev-immunol-061020-053707.

25. Dudziak, D., Kamphorst, A.O., Heidkamp, G.F., Buchholz, V.R., Trumpfheller, C., Yamazaki, S., Cheong, C., Liu, K., Lee, H.W., Park, C.G., et al. (2007). Differential antigen processing by dendritic cell subsets in vivo. Science *315*, 107–111. https://doi.org/10.1126/science.1136080.

26. Li, J., Lu, E., Yi, T., and Cyster, J.G. (2016). EBI2 augments Tfh cell fate by promoting interaction with IL-2-quenching dendritic cells. Nature *533*, 110–114. https://doi.org/10.1038/nature17947.

27. Choi, Y.S., Kageyama, R., Eto, D., Escobar, T.C., Johnston, R.J., Monticelli, L., Lao, C., and Crotty, S. (2011). ICOS receptor instructs T follicular helper cell versus effector cell differentiation via induction of the transcriptional repressor Bcl6. Immunity *34*, 932–946. https://doi.org/10.1016/j.immuni.2011.03.023.

28. Crotty, S. (2014). T follicular helper cell differentiation, function, and roles in disease. Immunity *41*, 529–542. https://doi.org/10.1016/j.immuni.2014.10.004.

29. Logue, E.C., Bakkour, S., Murphy, M.M., Nolla, H., and Sha, W.C. (2006). ICOS-induced B7h shedding on B cells is inhibited by TLR7/8 and TLR9. J. Immunol. *177*, 2356–2364. https://doi.org/10.4049/jimmunol.177.4.2356.

30. Zhang, X., Wang, Y., Song, J., Gerwien, H., Chuquisana, O., Chashchina, A., Denz, C., and Sorokin, L. (2020). The endothelial basement membrane acts as a checkpoint for entry of pathogenic T cells into the brain. J. Exp. Med. *217*, e20191339. https://doi.org/10.1084/jem.20191339.

31. Sasaki, T., and Timpl, R. (2001). Domain IVa of laminin alpha5 chain is cell-adhesive and binds beta1 and alphaVbeta3 integrins through Arg-Gly-Asp. FEBS Lett. *509*, 181–185.

32. Huang, H.Y., Rivas-Caicedo, A., Renevey, F., Cannelle, H., Peranzoni, E., Scarpellino, L., Hardie, D.L., Pommier, A., Schaeuble, K., Favre, S., et al. (2018). Identification of a new subset of lymph node stromal cells involved in regulating plasma cell homeostasis. Proc. Natl. Acad. Sci. USA *115*, E6826–E6835. https://doi.org/10.1073/pnas.1712628115.

33. Mii, Y., and Taira, M. (2011). Secreted Wnt "inhibitors" are not just inhibitors: regulation of extracellular Wnt by secreted Frizzled-related proteins. Dev. Growth Differ. *53*, 911–923. https://doi.org/10.1111/j.1440-169X.2011.01299.x.

34. Siegert, S., Huang, H.Y., Yang, C.Y., Scarpellino, L., Carrie, L., Essex, S., Nelson, P.J., Heikenwalder, M., Acha-Orbea, H., Buckley, C.D., et al. (2011). Fibroblastic reticular cells from lymph nodes attenuate T cell expansion by producing nitric oxide. PLoS One *6*, e27618. https://doi.org/10.1371/journal.pone.0027618.

35. Yang, C.Y., Vogt, T.K., Favre, S., Scarpellino, L., Huang, H.Y., Tacchini-Cottier, F., and Luther, S.A. (2014). Trapping of naive lymphocytes triggers rapid growth and remodeling of the fibroblast network in reactive murine lymph nodes. Proc. Natl. Acad. Sci. USA *111*, E109–E118. https://doi.org/10.1073/pnas.1312585111.

36. Martinez, V.G., Pankova, V., Krasny, L., Singh, T., Makris, S., White, I.J., Benjamin, A.C., Dertschnig, S., Horsnell, H.L., Kriston-Vizi, J., et al. (2019). Fibroblastic reticular cells control conduit matrix deposition during lymph node expansion. Cell Rep. *29*, 2810–2822.e5. https://doi.org/10.1016/j.celrep.2019.10.103.

37. Sixt, M., Engelhardt, B., Pausch, F., Hallmann, R., Wendler, O., and Sorokin, L.M. (2001). Endothelial cell laminin isoforms, laminin 8 and 10, play decisive roles in in T-cell recruitment across the blood-brain-barrier in an experimental autoimmune encephalitis model (EAE). J. Cell Biol. *153*, 933–946.

38. Ushiki, T., Ohtani, O., and Abe, K. (1995). Scanning electron microscopic studies of reticular framework in the rat mesenteric lymph node. Anat. Rec. *241*, 113–122.

39. Siegert, S., and Luther, S.A. (2012). Positive and negative regulation of T cell responses by fibroblastic reticular cells within paracortical regions of lymph nodes. Front. Immunol. *3*, 285. https://doi.org/10.3389/fimmu.2012.00285.

40. Bajénoff, M., Glaichenhaus, N., and Germain, R.N. (2008). Fibroblastic reticular cells guide T lymphocyte entry into and migration within the splenic T cell zone. J. Immunol. *181*, 3947–3954.

41. Cheng, P., Zhou, J., and Gabrilovich, D. (2010). Regulation of dendritic cell differentiation and function by Notch and Wnt pathways. Immunol.Rev. *234*, 105–119. https://doi.org/10.1111/j.0105-2896.2009.00871.x.

42. Oderup, C., LaJevic, M., and Butcher, E.C. (2013). Canonical and noncanonical Wnt proteins program dendritic cell responses for tolerance. J. Immunol. *190*, 6126–6134. https://doi.org/10.4049/jimmunol.1203002.

43. Suryawanshi, A., Tadagavadi, R.K., Swafford, D., and Manicassamy, S. (2016). Modulation of inflammatory responses by wnt/beta-catenin signaling in dendritic cells: anovel immunotherapy target for autoimmunity and cancer. Front. Immunol. *7*, 460. https://doi.org/10.3389/fimmu.2016.00460.

44. Swafford, D., and Manicassamy, S. (2015). Wnt signaling in dendritic cells: its role in regulation of immunity and tolerance. Discov. Med. *19*, 303–310.

45. Xu, W.D., Wang, J., Yuan, T.L., Li, Y.H., Yang, H., Liu, Y., Zhao, Y., and Herrmann, M. (2016). Interactions between canonical Wnt signaling pathway and MAPK pathway regulate differentiation, maturation and function of dendritic cells. Cell.Immunol. *310*, 170–177. https://doi.org/10.1016/j.cellimm.2016.09.006.

46. Kawano, Y., and Kypta, R. (2003). Secreted antagonists of the Wnt signalling pathway. J. Cell Sci. *116*, 2627–2634. https://doi.org/10.1242/jcs.00623.

47. Sixt, M., Hallmann, R., Wendler, O., Scharffetter-Kochanek, K., and Sorokin, L.M. (2001). Cell adhesion and migration properties of b2-integrin negative, polymorphonuclear granulocytes (PMN) on defined extracellular matrix molecules: relevance for leukocyte extravasation. J. Biol. Chem. *276*, 18878–18887.

48. Foo, S.S., Turner, C.J., Adams, S., Compagni, A., Aubyn, D., Kogata, N., Lindblom, P., Shani, M., Zicha, D., and Adams, R.H. (2006). Ephrin-B2 controls cell motility and adhesion during blood-vessel-wall assembly. Cell *124*, 161–173. https://doi.org/10.1016/j.cell.2005.10.034.

49. Muzumdar, M.D., Tasic, B., Miyamichi, K., Li, L., and Luo, L. (2007). A global double-fluorescent Cre reporter mouse. Genesis *45*, 593–605. https://doi.org/10.1002/dvg.20335.

50. Barnden, M.J., Allison, J., Heath, W.R., and Carbone, F.R. (1998). Defective TCR expression in transgenic mice constructed using cDNA-based alpha- and beta-chain genes under the control of heterologous regulatory elements. Immunol. Cell Biol. *76*, 34–40. https://doi.org/10.1046/j.1440-1711.1998.00709.x.

51. Bemark, M., Hazanov, H., Strömberg, A., Komban, R., Holmqvist, J., Köster, S., Mattsson, J., Sikora, P., Mehr, R., and Lycke, N.Y. (2016). Limited clonal relatedness between gut IgA plasma cells and memory B cells after oral immunization. Nat. Commun. *7*, 12698. https://doi.org/10.1038/ncomms12698.

52. Georges-Labouesse, E., Messaddeq, N., Yehia, G., Cadalbert, L., Dierich, A., and Le Meur, M. (1996). Absence of integrin a6 leads to epidermolysis bullosa and neonatal death in mice. Nat. Genet. *13*, 370–373.

53. Wu, C., Ivars, F., Anderson, P., Hallmann, R., Vestweber, D., Nilsson, P., Robenek, H., Tryggvason, K., Song, J., Korpos, E., et al.

(2009). Endothelial basement membrane laminin alpha5 selectively inhibits T lymphocyte extravasation into the brain. Nat. Med. *15*, 519–527.

54. Künneken, K., Pohlentz, G., Schmidt-Hederich, A., Odenthal, U., Smyth, N., Peter-Katalinic, J., Bruckner, P., and Eble, J.A. (2004). Recombinant human laminin-5 domains.Effects of heterotrimerization, proteolytic processing, and N-glycosylation on alpha3beta1 integrin binding. J. Biol. Chem. *279*, 5184–5193.

55. Miyazaki, T., Futaki, S., Hasegawa, K., Kawasaki, M., Sanzen, N., Hayashi, M., Kawase, E., Sekiguchi, K., Nakatsuji, N., and Suemori, H. (2008). Recombinant human laminin isoforms can support the undifferentiated growth of human embryonic stem cells. Biochem.Biophys. Res. Commun. *375*, 27–32. https://doi.org/10.1016/j.bbrc.2008.07.111.

56. Vuento, M., and Vaheri, A. (1979). Purification of fibronectin from human plasma by affinity chromatography under non-denaturing conditions. Biochem. J. *183*, 331–337.

57. Butler, A., Hoffman, P., Smibert, P., Papalexi, E., and Satija, R. (2018). Integrating single-cell transcriptomic data across different conditions, technologies, and species. Nat. Biotechnol. *36*, 411–420. https://doi.org/10.1038/nbt.4096.

58. Stuart, T., Butler, A., Hoffman, P., Hafemeister, C., Papalexi, E., Mauck, W.M., 3rd, Hao, Y., Stoeckius, M., Smibert, P., and Satija, R. (2019). Comprehensive integration of single-cell data. Cell *177*, 1888–1902.e21. https://doi.org/10.1016/j.cell.2019.05.031.

STAR★METHODS

KEY RESOURCES TABLE

REAGENT or RESOURCE	SOURCE	IDENTIFIER
Antibodies		
Pan-laminin (455)	Sixt et al.[37]	Antibody 455
Laminin α5	Sorokin et al.[20]; Sixt et al.[37]	Clone 4G6
Laminin α5	Sorokin et al.[20]; Sixt et al.[37]	Antibody 405
Laminin α5	Sorokin et al.[20]; Sixt et al.[37]	Antibody 504
Laminin β1	Sixt et al.[47]	Clone 3A4
Laminin β2	Sixt et al.[47]	Antibody 489
Laminin γ1	Sixt et al.[47]	Clone 3E10
Laminin γ3	Li et al.[21]	Antibody R96
Lntegrin α6	R&D Systems	Clone GoH3; Cat # MAB13501; RRID: AB_2128311
B220	R&D Systems	Clone RA3-6B2, Cat # MAB1217; RRID: AB_357537
CD11b/MAC-1	R&D Systems	Clone M1/70; Cat # MAB1124; RRID: AB_2128083
CD11c	Biolegend	Clone N418; Cat # 117309; RRID: AB_313778
syndecan-1/CD138	R&D Systems	Clone AF2780; Cat #AF2780; RRID: AB_442186
CD4	Biolegend	Clone H129.19; Cat # 130302; RRID: AB_1279242
CD25	Fisher Scientific	Clone 4C7; Cat # MA515653
CD275/ICOSL	Biolegend	Clone HK5.3; Cat # 107411; RRID: AB_2832361
ICOS	Biolegend	Clone 7E.17G9; Cat # 177413
CD279/PD-1	ThermoFisher Scientific	Clone J43; Cat # 14-9985-82; RRID: AB_468664
CD31/PECAM-1	Biolegend	Clone MEC13.3; Cat # 102501;RRID: AB_312908
IL-21	ThermoFisher Scientific	Clone FFA21; Cat # 16-7211-82; RRID: AB_1963610
BCL-6	eBioscience	Clone GI191E; Cat # 14-9887; RRID: AB_2865498
CD45	R&D Systems	Clone 30F11; Cat # MAB114; RRID: AB_357485
CD45.1	R&D Systems	Clone A20; Cat #553038
FAS/CD95	ThermoFisher Scientific	Clone 15A7; Cat # A16388
IgG1	Fisher Scientific	Clone R3-34; Cat # 15866748
CXCR5	BD Biosciences	Clone 2G8; Cat # 551960;RRID:AB_394301
ERTR7	BMA Biomedicals	Clone ERTR7; Cat # T-2109
FoxP3	ThermoFisher Scientific	Clone FJK-16s; Cat #14-5773-82
GL-7	ThermoFisher Scientific	Clone gl7; Cat # 14-5381-82
MHCII	ThermoFisher Scientific	Clone M5/114.15.2; Cat # 17-5321-82; RRID:AB_469455
PDGF-receptor-β	Iowa Hybridoma Bank	Clone APB5

Continued

REAGENT or RESOURCE	SOURCE	IDENTIFIER
peripheral node addressin	ThermoFisher Scientific	Clone MECA79; Cat # 53-6036-80; RRID:AB_10805867
gp38/podoplanin	ThermoFisher Scientific	Clone eBio8.1.1; Cat # 53-5381-82; RRID:AB_1106990
perlecan	ThermoFisher Scientific	Clone A7L6; Cat # MA5-14641; RRID:AB_10985966
CD19	BD Biosciences	Clone ID3; Cat # 553783; RRID:AB_395047
OTII TCR	BD Biosciences	Clone MR9-4; Cat # 553188; RRID:AB_394696
CD16/CD32	BD Biosciences	Clone 2.4G2; Cat #565502; RRID:AB_2739269
Chemicals, peptides, and recombinant proteins		
mini-laminin 511	Takaa Bio, USA	iMatrix-511; Cat #T304
Critical commercial assays		
Clonotyping System Kit	Southern Biotech	Cat # 5300-05
EasySep Mouse B-cell isolation kit	Stem Cell Technologies	Cat # 19854A
RNAscope® Multiplex Fluorescent Reagent Kit v2 Assay	ACD Bio-techne	Cat # 323100
Experimental models: Organisms/strains		
pdgfrb-cre::Lama5^{fl/fl}	Lead contact	*pdgfrb-cre::Lama5^{fl/fl}*
Oligonucleotides		
Chemokine (C-C motif) ligand 19 (*Ccl19*)	GGGGTGCTAATGATGCGGAA CCTTAGTGTGGTGAACACAACA	
Interleukin 7 (*Il7*)	TTCCTCCACTGATCCTTGTTCT AGCAGCTTCCTTTGTATCATCAC	
Cholesterol 25-hydroxylase (*Ch25h*)	TGCTACAACGGTTCGGAGC AGAAGCCCACGTAAGTGATGAT	
Cytochrome P450, family 7, subfamily b, polypeptide 1 (*Cyp7b1*)	GGAGCCACGACCCTAGATG TGCCAAGATAAGGAAGCCAAC	
Kruppel-like factor 2 (*Klf2*)	CTCAGCGAGCCTATCTTGCC CACGTTGTTTAGGTCCTCATCC	
Secreted frizzled-related protein 2 (*Sfrp2*)	CGTGGGCTCTTCCTCTTCG ATGTTCTGGTACTCGATGCCG	
Transcription factor 1, T-cell specific (*Tcf1*)	AGCTTTCTCCACTCTACGAACA AATCCAGAGAGATCGGGGGTC	
BCL6	CCGGCACGCTAGTGATGTT TGTCTTATGGGCTCTAAACTGCT	
TGF-β	CTCCCGTGGCTTCTAGTGC GCCTTAGTTTGGACAGGATCTG	
ICOS	TCCAGCAGTTAAAAATGCGATTG ATCCTCCACTAAGGTTCCTTTCT	
CD40L	CCTTGCTGAACTGTGAGGAGA CTTCGCTTACAACGTGTGCT	
CCR7	TGTACGAGTCGGTGTGCTTC GGTAGGTATCCGTCATGGTCTTG	
FasL	TCCGTGAGTTCACCAACCAAA GGGGGTTCCCTGTTAAATGGG	

Continued

REAGENT or RESOURCE	SOURCE	IDENTIFIER
Interleukin21 (*Il21*)	GGACCCTTGTCTGTCTGGTAG	
	TGTGGAGCTGATAGAAGTTCAGG	
Interleukin2 receptor-α (*Il2ra*	AACCATAGTACCCAGTTGTCGG	
	TCCTAAGCAACGCATATAGACCA	
Software and algorithms		
Volocity 6.3	PerkinElmer	

RESOURCE AVAILABILITY

Lead contact

Further information and requests for resources and reagents should be directed to and will be fulfilled by the lead contact, Lydia Sorokin (sorokin@uni-muenster.de).

Materials availability

A laminin α5 reticular fibroblast cell knockout mouse was generated by crossing the *Lama5*^{fl/fl} mouse[2] with the PDGFreceptor-β-cre recombinase mouse,[48] and is referred to as *pdgfrb-cre::Lama5*^{fl/fl}; it is available through the lead contact and is listed in the key resources table. This study did not generate any other new unique reagents and employed materials that were already available.

Data and code availability

All data reported in this paper will be shared by the lead contact upon request.

This paper does not report original code.

Any additional information required to reanalyze the data reported in this paper is available from the lead contact upon request.

EXPERIMENTAL MODEL AND SUBJECT DETAILS

Equal numbers of male and female mice on a C57BL/6 background were used at 8–15 weeks of age. Animal breeding and experiments were conducted according to the German Animal Welfare and ARRIVE guidelines, and were approved by the Animal Ethics Committee of the University of Muenster, Germany.

pdgfrb-cre::Lama5^{fl/fl} and control *Lama5*^{fl/fl} littermates were employed; the latter are referred to as WT controls. Ovalbumin-specific TCR-transgenic OT-II-Tomato mice were obtained by crossing the OTII mice with a global tandem-dimer tomato mouse.[49,50] 4-Hydroxy-3-nitrophenylacetyl (NP)-specific B-cell receptor knock-in B1-8[high]GFP mice[51] were used for adoptive transfer experiments. Bone marrow from *Itga6*[−/−52] or WT littermates were transferred to irradiated WT hosts for the generation of bone marrow chimeric mice.[53]

METHOD DETAILS

Immunization/antibody response

To analyze the immune response, WT or *pdgfrb-cre::Lama5*^{fl/fl} mice were immunized by subcutaneous injections of 50 μg OVA$_{323-339}$ or NP-CG in complete Freund's adjuvant (1:2 mixture). At 1 week after immunization, serum antibody titers were measured using the Clonotyping System Kit (Southern Biotech).

Adoptive transfer

CD4^{+}T-cells were isolated from spleens of OT-II-Tomato mice; NP-specific-GFP expressing B-cells from B1-8^{high}GFP mice were prepared by depletion of non-B-cells and vκ-expressing cells using EasySep Mouse B-cell isolation kit (Stem Cell Technologies) supplemented with 2 mg anti-mouse κ chain biotinylated antibody (BD Biosciences). CD4^{+}T-cells (5×10^6) were transferred with or without B1-8^{high}GFP cells to 8- to 9-week-old, sex matched recipients and the recipient mice were immunized by subcutaneous injection

with 50 μg NP-OVA in complete Freund's adjuvant. Analysis of the transferred cells in the lymph nodes at day 3 after transfer involved sectioning and staining, or flow cytometry. Antibodies to B220, TCR-β and laminin α5 (4G6),[20] pan-laminin or ERTR7 were used to immunofluorescently stain sections to define the B-cell and T-cell zones and the RF network.

Immunofluorescence

Lymph nodes were frozen in TissueTek (Miles Laboratories); cryostat sections (10–20 μm) were fixed for 10 min in −20°C methanol. Lymph nodes containing transferred OT-II-Tomato cells and B1-8[high]-GFP cells were fixed in 2% PFA for 30 minat 4°C before freezing in TissueTek. Sections were blocked in 1% BSA (in PBS) and incubated overnight at 4°C with primary antibodies. Following washing, sections were incubated for 1h at room temperature with fluorescently labeled secondary antibodies. Specimens were examined using a Zeiss AxioImager microscope and documented using Hamamatsu ORCA ER camera or with a Zeiss LSM 700 confocal laser scanning microscope. Image analyses were performed with the Volocity 6.3 program (PerkinElmer). Stereological analyses were performed on 5 sections each from 4 mice; distances of OTII-Tomato T-cells and B-8[high]-GFP B-cells to the follicle border were measured using the quantification module of Volocity 6.3. Follicles were identified using DAPI nuclear staining; B- and T-cells were identified based on intensity of the fluorescent signal and cell size (10–15 μm). For *in vivo* localization of CD11b^{+}CD11c^{+} DCs, relative to the follicle border, similar stereological analyses were performed on sections stained for CD11b, CD11c, pan-laminin to identify RFs, and DAPI. In the latter case we additionally calculated relative frequency distribution of double-positive cells, at defined distances from the follicle border. Prism generates an automated interval width (distance from follicle border) according to the sample size. Data are expressed as a percent of cells in a particular interval.

Flow cytometry

Single cell suspensions of lymph node cells were obtained by sieving through a 70 μm filter. Lymph node cells (1×10^6) were stained for markers of GC B-cells (CD19^{+}GL-7^{+} Fas^{+}) or Tfh-cells (CD4^{+}CXCR5^{+}PD-1^{+}ICOS^{+}) by first blocking Fc-receptors with CD16/CD32 antibody (BD Biosciences). Intracellular staining was performed using the Cytofix/Cytoperm kit (BD Biosciences) to identify the FoxP3 expressing subset in the Tfh-cells. To isolate DCs, lymph nodes were minced and digested in DMEM medium containing 1% FCS and 1 mg/ml collagenase-D (Sigma) for 30 min before sieving through a 100 μm sieve. Resident CD11b^{+}CD11c^{+}CD4^{+}CD25^{+} cDC2s were detected using flow cytometry using a FACS-Calibur or FACS-Celesta (Becton Dickinson) and data were analyzed using FlowJo (Treestar).

Antibodies employed

Antibodies employed in immunofluorescence staining and/or flow cytometry are listed in the key resources table.

DC cell adhesion assay

Purified human placental laminin 511[47]; recombinant laminin α5 domain IVa[31]; mini-laminin 511 composed of the C-terminal sequences of laminin α5, β1 and γ1 chains (Takaa Bio, USA)[54,55]; human serum fibronectin[56] were employed as substrates. Substrates were plated onto 24-well plates at 10 μg/ml by overnight incubation at 4°C, non-specific binding was blocked for 30 minat 37°C using 1% BSA in PBS. To isolate DCs, lymph nodes were dissected into small pieces and digested in HEPES buffer containing 2% FCS, 2 mg/ml Collagenase D (Sigma) and 20 μg/ml DNase I (Sigma) at 37°C for 30 minutes. After filtering through a 100 μm cell strainer, DCs were isolated using anti-CD11c MACS microbeads (Miltenyi). 2×10^6 cells were added/24-well and incubated at 37°C for 90 mins; after washing with PBS, adherent cells were analysed by flow cytometry for CD11c^{+}Cd11b^{+} cells. For inhibition studies, cells were incubated with 20 μg/ml GoH3 antibody or isotype control.

BrdU incorporation

WT and *pdgfrb-cre::Lama5^{fl/fl}* mice were immunized with NP-CG. BrdU was injected i.p. 16 hours before the mice were scarified. Draining lymph nodes were isolated and analyzed for BrdU incorporation in Tfh cells (CD4^{+}CXCR5^{+}) and cDC2 cells (CXCR5- CD4^{+}CD11c^{+}) by flow cytometry.

FRC and Tfh-cell sorting and qPCR analyses

Single cell suspensions were obtained by sieving lymph nodes through a 70 μm filter; CD4$^+$CXCR5$^+$PD-1$^+$Tfh-cells were sorted using a FACS-Aria. To isolate FRCs, lymph nodes were dissected into small pieces and digested in HEPES buffer containing 2% FCS, 2 mg/ml Collagenase D (Sigma) and 20 μg/ml DNase I (Sigma) at 37°C for 30 minutes. After filtering through a 100 μm cell strainer, leukocytes were depleted with anti-CD45 MACS microbeads (Miltenyi). The CD45 depleted cells were stained with antibodies against CD45, CD31, PDGF-receptor-β and gp38 for flow cytometry sorting using a FACS-Aria.

Total RNA was extracted from lymph nodes with RNeasy kit (QIAGEN) and cDNA was obtained using the Omniscript RT kit (QIAGEN). Quantitative-PCR was performed using the primers for fibroblastic reticular cells (*Ccl19, Il17, Ch25h, Cyp7b1, Klf2, Sfrp2*) and TfH cells (*Tcf1, Bcl6, Tgfb,Icos, CD40L, Ccr7, FasL, Il21, Il2ra*) listed in the key resources table. Fold change of gene expression are shown as 2$^{-\Delta\Delta CT}$ compared to Topo gene as a reference.

scRNA analysis

Data from Rodda et al., 2018[13] were accessed at GEO: GSE112903. R package Seurat[57,58] was used for data analyses. Count matrices were normalized using the SCTransform pipeline (https://satijalab.org/seurat/v3.1/sctransform_vignette.html). We determined 15 principal components (PC) and performed dimensionality reduction and cluster analysis with a resolution parameter of 0.25. A differential expression analysis was performed on each cluster and the results were visualized using UMAP. Clusters were assigned cell type identity based on already known markers.[13] FRC clusters were segregated into *Ccl19*$^+$ and *Ccl19*$^-$ sub-populations and a feature plot was used to define the gene expression patterns in these two populations. Dot plots were used to demonstrate the expression pattern and level of expression of specific genes.

RNAscope

Fresh frozen tissue sections were fixed and dehydrated before proceeding to the RNAscope assay (RNAscope® Multiplex Fluorescent Reagent Kit v2 Assay, ACD Biotechne). IgM antibody staining was performed using co-ISH with the Ch25h RNAscope probe (424561).

QUANTIFICATION AND STATISTICAL ANALYSIS

Data were analysed using Prism software (GraphPad). The Mann Whitney U test was used to compare conditions unless otherwise stated. Data are expressed as mean values ±standard deviation. *P<0.05, **P<0.01, ***P<0.001, ****P<0.0001.